Table 2. Multivariate analysis of GVHD, outcome and significant factors

	Hazard ratio	*95%CI*	P-*value*
Grade II-IV acute GVHD			
Body mass index			
Underweight	0.94	0.86–1.03	0.21
Normal	1		
Overweight	1.13	1.03–1.24	0.011
Obesity	0.94	0.74–1.20	0.64
GVHD prophylaxis			
CSP-based	1		
TAC-based	0.84	0.77–0.90	< 0.001
HLA mismatch			
Match	1		
Mismatch	1.56	1.44–1.70	< 0.001
Performance status			
0–1	1		
2–4	0.74	0.66–0.83	< 0.001
Conditioning regimen			
Myeloablative	1		
Reduced-intensity	0.85	0.79–0.91	< 0.001
Stem cell source			
Related BM	1		
Related PBSC	1.24	1.12–1.38	< 0.001
Unrelated BM	1.62	1.47–1.78	< 0.001
Disease risk			
Standard	1		
High	1.13	1.06–1.21	< 0.001
Year of transplant			
< 2007	1		
⩾ 2007	0.85	0.80–0.91	< 0.001
Grade III–IV acute GVHD			
Body mass index			
Underweight	0.96	0.82–1.11	0.60
Normal	1		
Overweight	1.27	1.10–1.48	0.002
Obesity	1.17	0.81–1.70	>0.41
HLA mismatch			
Match	1		
Mismatch	1.45	1.28–1.65	< 0.001
Stem cell source			
Related BM	1		
Related PBSC	1.61	1.34–1.93	< 0.001
Unrelated BM	1.52	1.29–1.79	< 0.001
Disease risk			
Standard	1		
High	1.26	1.13–1.41	< 0.001
Year of transplant			
< 2007	1		
⩾ 2007	0.80	0.72–0.89	< 0.001

Abbreviation: TAC = tacrolimus.

Supplementary Table 1). The cumulative incidence of chronic GVHD at 2 years was 32.5% in the underweight, 35.8% in normal, 36.6% in overweight and 40.1% in obese groups ($P = 0.042$, Figure 1e). In a multivariate analysis, BMI was not a significant risk factor for chronic GVHD. The cumulative incidence of extensive chronic GVHD was 19.9% in the underweight, 23.7% in normal, 24.9% in overweight and 28.4% in obese groups ($P = 0.001$, Figure 1f). A multivariate analysis showed that obesity was associated with an increased risk of extensive chronic GVHD (HR 1.32, 95%CI 1.01–1.74, $P = 0.043$, Supplementary Table 1).

The cumulative incidence of NRM at 2 years was 19.5% in the underweight, 21.9% in normal, 25.1% in overweight and 23.0% in obese groups ($P = 0.002$, Figure 2a). A multivariate analysis showed that overweight and obesity were each associated with an increased risk of NRM (HR 1.19, 95%CI 1.06–1.33, $P = 0.004$; HR 1.43, 95%CI 1.08–1.88, $P = 0.012$, Table 3). Only 30 of the 12 050 patients had a BMI > 35 kg/m^2 (0.25%). In these patients, the cumulative incidence of NRM at 2 years was 25.6%. The cumulative incidence of infection-related NRM at 2 years was 5.7% in the underweight, 6.3% in normal, 7.7% in overweight and 5.2% in obese groups ($P = 0.021$, Figure 2b). A multivariate analysis showed that overweight was associated with an increased risk of infection-related NRM (HR 1.34, 95% CI 1.09–1.64, $P = 0.006$). The cumulative incidence of GVHD-related NRM at 2 years was 2.3% in the underweight, 3.1% in normal, 4.5% in overweight and 5.1% in obese groups ($P = 0.002$, Figure 2c). A multivariate analysis showed that obesity was associated with an increased risk of GVHD-related NRM (HR 2.15, 95% CI 1.20–3.86, $P = 0.010$). In patients who developed grade II–IV acute GVHD, the cumulative incidence of 2-year NRM after acute GVHD was 23.8% in the underweight, 28.8% in normal, 32.6% in overweight and 34.1% in obese groups ($P = 0.001$). A multivariate analysis showed that overweight and obesity were each associated with an increased risk of NRM in patients who developed grade II–IV acute GVHD (HR 1.18, 95% CI 1.01–1.39, $P = 0.040$; HR 1.62, 95%CI 1.09–2.42, $P = 0.018$). In patients who developed grade III–IV acute GVHD, the cumulative incidence of 2-year NRM after acute GVHD was 39.7% in the underweight, 49.4% in normal, 53.8% in overweight and 59.0% in obese groups ($P = 0.003$). A multivariate analysis showed that underweight and obesity were associated with a decreased and increased risk of NRM, respectively, in patients who developed grade III–IV acute GVHD (HR 0.72, 95% CI 0.56–0.92, $P = 0.009$; HR 1.65, 95% CI 1.01–2.71, $P = 0.048$).

We also assessed the impact of BMI on NRM in a multivariate analysis that included hematopoietic cell transplant-specific comorbidity index scores. In a multivariate analysis that included hematopoietic cell transplant-specific comorbidity index (0 points vs 1–2 points vs ⩾ 3 points), overweight and obesity were each still associated with an increased risk of NRM (HR 1.26, 95% CI 1.05–1.50, $P = 0.012$; HR 1.54, 95% CI 1.05–2.26, $P = 0.029$).

The cumulative incidence of relapse/progression was 35.6% in the underweight, 30.5% in normal, 23.9% in overweight and 22.6% in obese groups ($P < 0.0001$, Figure 2d). A multivariate analysis showed that underweight was associated with a higher risk of relapse (HR 1.16, 95% CI 1.06–1.28, $P = 0.002$), and overweight and obesity were each associated with a lower risk of relapse (HR 0.86, 95% CI 0.77–0.96, $P = 0.008$; HR 0.74, 95% CI 0.56–0.99, $P = 0.045$, Table 4). In patients with BMI ⩾ 35 kg/m^2, the cumulative incidence of relapse at 2 years was 18.4%. We conducted a subgroup analysis according to the underlying hematological malignancies. In patients with AML, the cumulative incidence of relapse/progression was 43.5% in the underweight, 35.5% in normal, 28.3% in overweight and 28.6% in obese groups ($P < 0.0001$). In patients with ALL, the cumulative incidence of relapse/progression was 31.9% in the underweight, 28.9% in normal, 21.8% in overweight and 22.1% in obese groups ($P = 0.091$).

The probability of OS at 2 years after allogeneic HSCT was 49.4% in the underweight, 53.0% in normal, 54.9% in overweight and 63.5% in obese groups ($P = 0.002$, Figure 2e). A multivariate analysis showed that underweight was associated with a worse OS than that in the normal group (HR 1.10, 95% CI 1.02–1.19, $P = 0.018$, Table 4).

We conducted a subgroup analysis according to the conditioning regimen. In patients who received a conventional CY plus TBI-

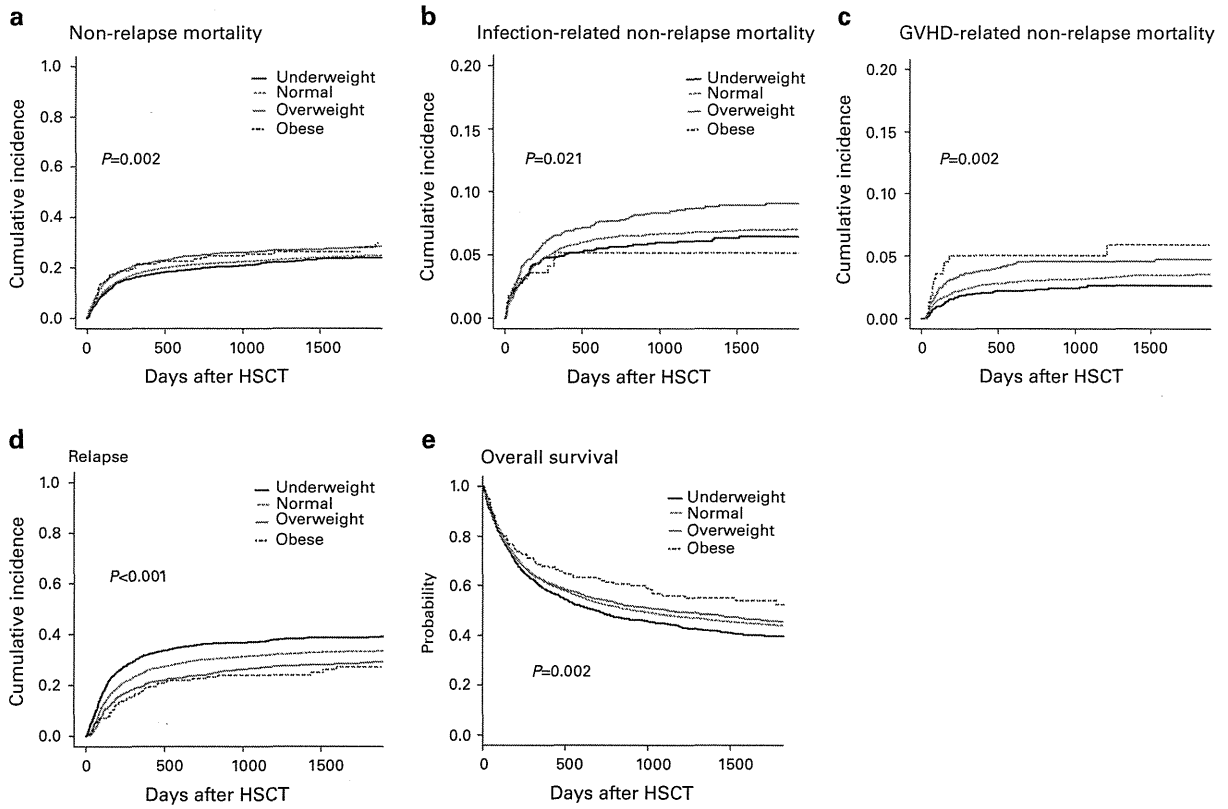

Figure 2. Cumulative incidence of (**a**) NRM (**a**), infection-related NRM (**b**), GVHD-related NRM (**c**) and relapse (**d**), probability of OS (**e**) grouped according to pretransplant BMI.

based myeloablative conditioning regimen, the cumulative incidence of relapse/progression was 33.6% in the underweight, 28.8% in normal, 23.1% in overweight and 23.6% in obese groups ($P < 0.0001$), and the cumulative incidence of NRM was 17.1% in the underweight, 21.0%in normal, 25.3% in overweight and 23.9% in obese groups ($P = 0.003$). In patients who received a BU plus CY-based myeloablative conditioning regimen, the cumulative incidence of relapse/progression was 38.9% in the underweight, 27.2% in normal, 20.7% in overweight and 13.5% in obese groups ($P = 0.001$), and the cumulative incidence of NRM was 18.9% in the underweight, 22.2% in normal, 25.8% in overweight and 17.1% in obese groups ($P = 0.47$). In patients who received a reduced-intensity conditioning regimen, the cumulative incidence of relapse/progression was 35.0% in the underweight, 33.2% in normal, 25.5% in overweight and 22.8% in obese groups ($P = 0.018$), and the cumulative incidence of NRM was 22.0% in the underweight, 21.7% in normal, 25.9% in overweight and 22.4% in obese groups ($P = 0.13$).

DISCUSSION

Here, we demonstrated that pretransplant BMI significantly influenced the post-transplant clinical outcome. To our knowledge, this is the largest study on the impact of pretransplant BMI after allogeneic HSCT. Our study showed that patients with a low BMI had the worst OS because of an increased risk of relapse, whereas patients with a high BMI had the highest NRM because of an increased risk of GVHD-related NRM.

Regarding the impact of obesity, Sorror *et al.*[3] reported that obesity (BMI > 35 kg/m^2) was associated with an increased risk of NRM. However, in Japan and many other countries, the prevalence of patients with BMI > 35 kg/m^2 is rather low, as shown in this study and previous reports.[1,5] A previous study showed that the mean BMIs in the US and Japan were 28 kg/m^2 and 22 kg/m^2, respectively, which shows that there is a huge difference in BMI between the two countries.[1] In the current study, only 30 of the 12 050 total patients had BMI > 35 kg/m^2 (0.25%). Although the risk of NRM in patients with BMI > 35 kg/m^2 tended to be higher than that in patients with normal BMI (2-year NRM 25.6% vs 21.9%), this difference was not statistically significant, possibly because of the limited number of patients. Theoretically, Japanese patients compared to Caucasian patients should have less GVHD because of less HLA gene variability and less obesity because of diet. Therefore, the findings of this study could be even more pronounced in Caucasian patients, which should be assessed using data of Caucasian patients.

In the current study, obese patients (BMI ⩾ 30 kg/m^2) had a higher risk of NRM, and particularly GVHD-related NRM, compared with those with normal BMI. In addition, obese patients had a worse outcome than those with normal BMI when patients developed grade II–IV or grade III–IV acute GVHD. One possible reason why obese patients had a higher risk of GVHD-related death is the higher incidences of hepatic and gut acute GVHD in comparison with patients with normal BMI, which have been reported to be associated with a poor response to GVHD therapy and an increased risk of NRM.[13–16] One hypothesis is that the greater tissue damage caused by the higher dose of chemotherapy in obese patients may contribute to the induction of cytokine storms, which leads to severe acute GVHD.[17] Another hypothesis is that the different immune status in obesity affects the functional status of immune cells after allogeneic HSCT. It has been reported that, in obese patients, the number of adipose tissue-resident immune cells, such as macrophages, CD8$^+$ T cells and IFN-γ Th1$^+$ cells, is increased, and the number of regulatory T cells is decreased.[18–20] Such an obesity-induced shift in adipose tissue-resident immune cells might increase the alloimmune reaction

Table 3. Multivariate analysis of NRM, outcome and significant factor

	Hazard ratio	*95%CI*	P-*value*
NRM			
Body mass index			
Underweight	0.93	0.83–1.06	0.28
Normal	1		
Overweight	1.19	1.06–1.33	0.004
Obesity	1.43	1.08–1.88	0.012
Age			
Age < 50	1		
Age ⩾ 50	1.62	1.47–1.77	< 0.001
HLA mismatch			
Match	1		
Mismatch	1.45	1.31–1.60	< 0.001
Sex combination			
Female to male	1.30	1.18–1.43	< 0.001
Others	1		
Performance status			
0–1	1		
2–4	1.44	1.26–1.63	< 0.001
Stem cell source			
Related BM	1		
Related PBSC	1.14	0.99–1.31	0.073
Unrelated BM	1.70	1.50–1.92	< 0.001
Conditioning regimen			
Myeloablative	1		
Reduced-intensity	0.90	0.81–0.99	0.027
Year of transplant			
< 2007	1		
⩾ 2007	0.72	0.67–0.79	< 0.001
Infection-related NRM			
Body mass index			
Underweight	0.9	0.71–1.13	0.35
Normal	1		
Overweight	1.34	1.09–1.64	0.006
Obesity	1.05	0.57–1.92	0.89
Age			
Age < 50	1		
Age ⩾ 50	1.82	1.56–2.13	< 0.001
HLA mismatch			
Match	1		
Mismatch	1.49	1.24–1.78	< 0.001
Sex combination			
Female to male	1.30	1.09–1.55	0.004
Others	1		
Performance status			
0–1	1		
2–4	1.45	1.16–1.80	0.001
Stem cell source			
Related BM	1		
Related PBSC	1.15	0.88–1.49	0.31
Unrelated BM	1.64	1.30–2.06	< 0.001
Year of transplant			
< 2007	1		
⩾ 2007	0.71	0.61–0.83	< 0.001
GVHD-related NRM			
Body mass index			
Underweight	0.79	0.55–1.12	0.18
Normal	1		
Overweight	1.26	0.93–1.72	0.14
Obesity	2.15	1.20–3.86	0.010
HLA mismatch			
Match	1		
Mismatch	1.44	1.11–1.87	0.007
Disease risk			
Standard	1		
High	1.44	1.15–1.82	0.002
Stem cell source			
Related BM	1		
Related PBSC	1.40	0.94–2.07	0.098
Unrelated BM	1.67	1.18–2.36	0.004
Year of transplant			
< 2007	1		
⩾ 2007	0.74	0.59–0.93	0.009

Abbreviation: NRM = non-relapse mortality.

after allogeneic HSCT as reported in the field of organ transplantation, as reviewed previously.[21] Intriguingly, previous studies have reported that Caucasian patients had an increased risk of acute GVHD compared to Asian patients.[22,23] The huge difference in BMI among races might at least partially influence the incidence of acute GVHD.

The obese patients in this study had a substantially increased risk of stage 2–4 acute GVHD in the liver (HR 2.00, 95% CI 1.26–3.17). Considering the mortality associated with hepatic acute GVHD, we should intervene to reduce the risk of hepatic acute GVHD in obese patients.[13–16] It is well-known that a prominent obesity-induced immune shift in the liver, so-called non-alcoholic steatohepatitis, causes inflammation in the liver, which might contribute to the subsequent increased risk of hepatic acute GVHD.[18,24] Practically, careful monitoring and early institution of high-dose immunosuppression are suggested. As a possible intervention, weight loss by diet and exercise could be a safe option, and has been shown to dose-dependently improve histological disease activity in non-alcoholic steatohepatitis associated with obesity.[25,26]

In terms of the impact of being underweight, several previous studies have also reported that being underweight was associated with a poor outcome after allogeneic HSCT.[4,27,28] Navarro *et al.*[4] has reported that OS in AML patients with BMI at transplant < 18 was inferior to that in patients with a normal BMI in patients who received stem cells from related donors, but not in the unrelated donor group. In terms of relapse, the relative risk of relapse was reduced for the overweight (relative risk 0.82, 95%CI 0.68–0.99, $P = 0.044$) and obese (relative risk 0.76, 95% CI 0.0.60–0.96, $P = 0.022$) groups. However, in terms of disease-free survival (Figure 2b in Navarro *et al.*[4]), there was a clear trend that the outcome in AML patients with BMI at transplant < 18 was inferior to that in patients with a normal BMI in patients who received stem cells from unrelated donors. The lack of statistical significance in unrelated HSCT might be because of a lack of power in the study (33 in 1801 patients). Underweight patients may have had more advanced disease compared with those with higher BMI, even though the proportion of patients with advanced disease was the same in the underweight and normal groups in this study. Shorter interval between diagnosis and transplant in the underweight group might suggest the aggressive nature of underlying disease. In a multivariate analysis, being underweight was associated with an increased risk of relapse independent of

Table 4. Multivariate analysis of relapse and OS, outcome and significant factor

	Hazard ratio	*95%CI*	P-*value*
Relapse			
Body mass index			
Underweight	1.16	1.06–1.28	0.002
Normal	1		
Overweight	0.86	0.77–0.96	0.008
Obesity	0.74	0.56–0.99	0.045
Age			
Age < 50	1		
Age ⩾ 50	1.11	1.03–1.20	0.001
Sex combination			
Female to male	0.89	0.81–0.97	0.007
Others	1		
Performance status			
0–1	1		
2–4	1.77	1.60–1.96	< 0.001
Conditioning regimen			
Myeloablative	1		
Reduced-intensity	0.86	0.80–0.93	< 0.001
Stem cell source			
Related BM	1		
Related PBSC	1.1	1.00–1.22	0.061
Unrelated BM	0.77	0.70–0.85	< 0.001
Disease risk			
Standard	1		
High	2.52	2.34–2.72	< 0.001
Year of transplant			
< 2007	1		
⩾ 2007	1.11	1.04–1.19	0.003
OS			
Body mass index			
Underweight	1.10	1.02–1.19	0.018
Normal	1		
Overweight	1.02	0.94–1.11	0.67
Obesity	0.95	0.76–1.19	0.67
Age			
Age < 50	1		
Age ⩾ 50	1.51	1.42–1.60	< 0.001
HLA mismatch			
Match	1		
Mismatch	1.33	1.25–1.43	< 0.001
Sex combination			
Female to male	1.10	1.03–1.18	0.005
Others	1		
Conditioning regimen			
Myeloablative	1		
Reduced-intensity	0.81	0.76–0.86	< 0.001
Performance status			
0–1	1		
2–4	2.31	2.14–2.49	< 0.001
Stem cell source			
Related BM	1		
Related PBSC	1.19	1.09–1.30	< 0.001
Unrelated BM	1.23	1.14–1.34	< 0.001
Year of transplant			
< 2007	1		
⩾ 2007	0.94	0.89–0.99	0.027

performance status and disease risk. When we performed a subgroup analysis that included only patients with high-risk disease, being underweight was still independently associated with a poor OS because of a significantly increased risk of relapse compared with the normal group (HR 1.11, 95% CI 1.01–1.22, $P = 0.027$). Furthermore, even when we grouped patients according to the conditioning regimen, the cumulative incidence of relapse was significantly higher in the underweight group compared with the other groups, irrespective of the type of the conditioning regimen. One possible explanation for why underweight patients had an increased risk of relapse is the insufficient dosage of chemotherapy compared with those in the other groups. In underweight patients, actual body weight is usually used to calculate the dose of chemotherapy. Therefore, the dose of chemotherapy in underweight patients should be lower than those in patients with normal or heavier body weight, considering the dose per ideal body weight. However, it is uncertain whether the adjusted dose of chemotherapy using an ideal body weight in patients with low BMI could lead to a better outcome without an increased risk of morbidities. In addition, several previous reports showed that the status of nutrition had an impact on the metabolism of the chemotherapeutic drugs.[29,30] For instance, nutritional status was reported to affect the level of cytochrome P450 enzymes which are responsible for the metabolism of the chemotherapeutic drugs. It was reported that there was a correlation between total body weight and plasma half-life of CY, which means that the concentration of CY is higher in obese patients compared with the normal weight patients.[31] Such changes in the metabolism of chemotherapeutic drugs might affect the risk of relapse and NRM in the setting of allogeneic HSCT.

An intervention that may improve the outcome is the amelioration of body weight loss before allogeneic HSCT. In general nutrition screening, BMI < 18.5 kg/m^2 is defined as an impaired nutritional status according to the European Society of Parenteral and Enteral Nutrition guidelines for 2002.[32] It may be possible to at least partially prevent pretransplant weight loss with some intervention including lifestyle modification, such as intensive nutritional support and exercise during induction and consolidation chemotherapy.[33,34] Exercise is important for maintaining skeletal muscle mass, and sufficient nutritional support is essential for preventing catabolism, since previous reports have demonstrated a high prevalence of sarcopenia before allogeneic HSCT.[33–35]

This study has some limitations. Because of the nature of the registry database, we were not able to assess the policies regarding adjustment of the conditioning regimen dose for patients with obesity, which will likely vary among the transplant centers. Another important limitation is that we included almost exclusively Japanese patients. Therefore, it is uncertain whether similar findings would be seen in other countries/regions. Our findings should be reassessed using other databases. Furthermore, because of the nature of the registry database, we were not able to assess the change of body weight and anthropometric measures before allogeneic HSCT. Although no standardized nutritional screening tool has been designed specifically for use in patients who undergo allogeneic HSCT, weight loss and anthropometric measures is in general regarded as an integral part of nutritional screening in most nutritional screening tool.[32,36,37] A recent study reported that pretransplant low arm muscle area was a stronger predictor than BMI of poor outcomes after HCT in children with hematologic malignancies.[38] The impact of pretransplant BMI, anthropometric measures and change of body weight should be assessed in the future studies.

In conclusion, we demonstrated that pretransplant BMI significantly affected the major post-transplant outcome. A prospective study to assess the impact of intervention including nutritional support and exercise is warranted.

CONFLICT OF INTEREST

The authors declare no conflict of interest.

ACKNOWLEDGEMENTS

We thank the medical, nursing, data-processing, laboratory and clinical staffs at the participating centers for their important contributions to this study and their dedicated care of the patients. This study was supported in part by grants from the Ministry of Health, Labor and Welfare, Japan.

REFERENCES

1 Finucane MM, Stevens GA, Cowan MJ, Danaei G, Lin JK, Paciorek CJ *et al.* National, regional, and global trends in body-mass index since 1980: systematic analysis of health examination surveys and epidemiological studies with 960 country-years and 9.1 million participants. *Lancet* 2011; **377**: 557–567.
2 Fearon K, Strasser F, Anker SD, Bosaeus I, Bruera E, Fainsinger RL *et al.* Definition and classification of cancer cachexia: an international consensus. *Lancet Oncol* 2011; **12**: 489–495.
3 Sorror ML, Maris MB, Storb R, Baron F, Sandmaier BM, Maloney DG *et al.* Hematopoietic cell transplantation (HCT)-specific comorbidity index: a new tool for risk assessment before allogeneic HCT. *Blood* 2005; **106**: 2912–2919.
4 Navarro WH, Agovi MA, Logan BR, Ballen K, Bolwell BJ, Frangoul H *et al.* Obesity does not preclude safe and effective myeloablative hematopoietic cell transplantation (HCT) for acute myelogenous leukemia (AML) in adults. *Biol Blood Marrow Transplant* 2010; **16**: 1442–1450.
5 Fuji S, Kim SW, Yoshimura K, Akiyama H, Okamoto S, Sao H *et al.* Possible association between obesity and posttransplantation complications including infectious diseases and acute graft-versus-host disease. *Biol Blood Marrow Transplant* 2009; **15**: 73–82.
6 Atsuta Y, Suzuki R, Yoshimi A, Gondo H, Tanaka J, Hiraoka A *et al.* Unification of hematopoietic stem cell transplantation registries in Japan and establishment of the TRUMP System. *Int J Hematol* 2007; **86**: 269–274.
7 WHO. Obesity: preventing and managing the global epidemic. Report of a WHO consultation. *World Health Organ Tech Rep Ser* 2000; **894**: 1–253.
8 Pi-Sunyer FX BD, Bouchard C, Carleton RA, Colditz GA, Dietz WH, Foreyt JP *et al.* Clinical Guidelines on the Identification, Evaluation, and Treatment of Overweight and Obesity in Adults--The Evidence Report. National Institutes of Health. *Obes Res* 1998; **6**(Suppl 2): 51S–209S.
9 Glucksberg H, Storb R, Fefer A, Buckner CD, Neiman PE, Clift RA *et al.* Clinical manifestations of graft-versus-host disease in human recipients of marrow from HL-A-matched sibling donors. *Transplantation* 1974; **18**: 295–304.
10 Przepiorka D, Weisdorf D, Martin P, Klingemann HG, Beatty P, Hows J *et al.* 1994Consensus Conference on Acute GVHD Grading. *Bone Marrow Transplant* 1995; **15**: 825–828.
11 Oken MM, Creech RH, Tormey DC, Horton J, Davis TE, McFadden ET *et al.* Toxicity and response criteria of the Eastern Cooperative Oncology Group. *Am J Clin Oncol* 1982; **5**: 649–655.
12 Kanda Y. Investigation of the freely available easy-to-use software 'EZR' for medical statistics. *Bone Marrow Transplant* 2013; **48**: 452–458.
13 Lee KH, Choi SJ, Lee JH, Lee JS, Kim WK, Lee KB *et al.* Prognostic factors identifiable at the time of onset of acute graft-versus-host disease after allogeneic hematopoietic cell transplantation. *Haematologica* 2005; **90**: 939–948.
14 Robin M, Porcher R, de Castro R, Fisher G, de Latour RP, Ribaud P *et al.* Initial liver involvement in acute GVHD is predictive for nonrelapse mortality. *Transplantation* 2009; **88**: 1131–1136.
15 Murata M, Nakasone H, Kanda J, Nakane T, Furukawa T, Fukuda T *et al.* Clinical factors predicting the response of acute graft-versus-host disease to corticosteroid therapy: an analysis from the GVHD Working Group of the Japan Society for Hematopoietic Cell Transplantation. *Biol Blood Marrow Transplant* 2013; **19**: 1183–1189.
16 Weisdorf D, Haake R, Blazar B, Miller W, McGlave P, Ramsay N *et al.* Treatment of moderate/severe acute graft-versus-host disease after allogeneic bone marrow transplantation: an analysis of clinical risk features and outcome. *Blood* 1990; **75**: 1024–1030.
17 Ferrara JL, Levine JE, Reddy P, Holler E. Graft-versus-host disease. *Lancet* 2009; **373**: 1550–1561.
18 Schipper HS, Prakken B, Kalkhoven E, Boes M. Adipose tissue-resident immune cells: key players in immunometabolism. *Trends Endocrinol Metab* 2012; **23**: 407–415.
19 Cai D, Yuan M, Frantz DF, Melendez PA, Hansen L, Lee J *et al.* Local and systemic insulin resistance resulting from hepatic activation of IKK-beta and NF-kappaB. *Nat Med* 2005; **11**: 183–190.
20 Conde J, Scotece M, Gomez R, Lopez V, Gomez-Reino JJ, Lago F *et al.* Adipokines: biofactors from white adipose tissue. A complex hub among inflammation, metabolism, and immunity. *Biofactors* 2011; **37**: 413–420.
21 Heinbokel T, Floerchinger B, Schmiderer A, Edtinger K, Liu G, Elkhal A *et al.* Obesity and its impact on transplantation and alloimmunity. *Transplantation* 2013; **96**: 10–16.
22 Oh H, Loberiza FR Jr, Zhang MJ, Ringden O, Akiyama H, Asai T *et al.* Comparison of graft-versus-host-disease and survival after HLA-identical sibling bone marrow transplantation in ethnic populations. *Blood* 2005; **105**: 1408–1416.
23 Hahn T, McCarthy PL Jr, Zhang MJ, Wang D, Arora M, Frangoul H *et al.* Risk factors for acute graft-versus-host disease after human leukocyte antigen-identical sibling transplants for adults with leukemia. *J Clin Oncol* 2008; **26**: 5728–5734.
24 Baffy G. Kupffer cells in non-alcoholic fatty liver disease: the emerging view. *J Hepatol* 2009; **51**: 212–223.
25 Tilg H, Moschen A. Weight loss: cornerstone in the treatment of non-alcoholic fatty liver disease. *Minerva Gastroenterol Dietol* 2010; **56**: 159–167.
26 Musso G, Cassader M, Rosina F, Gambino R. Impact of current treatments on liver disease, glucose metabolism and cardiovascular risk in non-alcoholic fatty liver disease (NAFLD): a systematic review and meta-analysis of randomised trials. *Diabetologia* 2012; **55**: 885–904.
27 Le Blanc K, Ringden O, Remberger M. A low body mass index is correlated with poor survival after allogeneic stem cell transplantation. *Haematologica* 2003; **88**: 1044–1052.
28 Deeg HJ, Seidel K, Bruemmer B, Pepe MS, Appelbaum FR. Impact of patient weight on non-relapse mortality after marrow transplantation. *Bone Marrow Transplant* 1995; **15**: 461–468.
29 Murry DJ, Riva L, Poplack DG. Impact of nutrition on pharmacokinetics of antineoplastic agents. *Int J Cancer Suppl* 1998; **11**: 48–51.
30 Boullata JI. Drug disposition in obesity and protein-energy malnutrition. *Proc Nutr Soc* 2010; **69**: 543–550.
31 Powis G, Reece P, Ahmann DL, Ingle JN. Effect of body weight on the pharmacokinetics of cyclophosphamide in breast cancer patients. *Cancer Chemother Pharmacol* 1987; **20**: 219–222.
32 Kondrup J, Allison SP, Elia M, Vellas B, Plauth M. Educational and Clinical Practice Committee, European Society of Parenteral and Enteral Nutrition (ESPEN) ESPEN guidelines for nutrition screening 2002. *Clin Nutr* 2003; **22**: 415–421.
33 Coss CC, Bohl CE, Dalton JT. Cancer cachexia therapy: a key weapon in the fight against cancer. *Curr Opin Clin Nutr Metab Care* 2011; **14**: 268–273.
34 Bosaeus I. Nutritional support in multimodal therapy for cancer cachexia. *Support Care Cancer* 2008; **16**: 447–451.
35 Morishita S, Kaida K, Tanaka T, Itani Y, Ikegame K, Okada M *et al.* Prevalence of sarcopenia and relevance of body composition, physiological function, fatigue, and health-related quality of life in patients before allogeneic hematopoietic stem cell transplantation. *Support Care Cancer* 2012; **20**: 3161–3168.
36 Kondrup J, Rasmussen HH, Hamberg O, Stanga Z. Nutritional risk screening (NRS 2002): a new method based on an analysis of controlled clinical trials. *Clin Nutr* 2003; **22**: 321–336.
37 Stratton RJ, Hackston A, Longmore D, Dixon R, Price S, Stroud M *et al.* Malnutrition in hospital outpatients and inpatients: prevalence, concurrent validity and ease of use of the 'malnutrition universal screening tool' ('MUST') for adults. *Br J Nutr* 2004; **92**: 799–808.
38 Hoffmeister PA, Storer BE, Macris PC, Carpenter PA, Baker KS. Relationship of body mass index and arm anthropometry to outcomes after pediatric allogeneic hematopoietic cell transplantation for hematologic malignancies. *Biol Blood Marrow Transplant* 2013; **19**: 1081–1086.

Supplementary Information accompanies this paper on Bone Marrow Transplantation website (http://www.nature.com/bmt)

Bone Marrow Transplantation (2015), 1–6

www.nature.com/bmt

ORIGINAL ARTICLE

Pre-transplant diabetes mellitus is a risk factor for non-relapse mortality, especially infection-related mortality, after allogeneic hematopoietic SCT

K Takano[1,2,10], S Fuji[1,10], N Uchida[3], H Ogawa[4], K Ohashi[5], T Eto[6], H Sakamaki[5], Y Morishima[7], K Kato[8], R Suzuki[9] and T Fukuda[1]

Diabetes mellitus (DM) is a factor in the hematopoietic cell transplantation-comorbidity index. However, the impact of pre-transplant DM on morbidity and cause-specific non-relapse mortality (NRM) remains unclear. We performed a retrospective study with registry data that included a total of 7626 patients who underwent their first allogeneic hematopoietic SCT (HSCT) between 2007 and 2010. The median age was 44 years (range 0–88). Compared with patients without pre-transplant DM (non-DM group, $n=7248$), patients with pre-transplant DM (DM group, $n=378$) were older and were more likely to have high-risk disease, a reduced-intensity conditioning regimen and GVHD prophylaxis using tacrolimus. Multivariate analyses showed that pre-transplant DM was associated with increased risks of NRM (hazard ratio (HR)1.46, 95% confidence interval (CI) 1.21–1.76, $P<0.01$) and infection-related NRM (HR 2.08, 95% CI 1.58–2.73, $P<0.01$). The presence of pre-transplant DM was associated with an increased risk of overall mortality in a multivariate analysis (HR 1.55, 95% CI 1.35–1.78, $P<0.01$). In conclusion, pre-transplant DM was a risk factor for NRM, particularly infection-related mortality, after allogeneic HSCT. To improve the clinical outcome in patients with DM, the benefits of strict infection control and appropriate glycemic control should be explored in future trials.

Bone Marrow Transplantation advance online publication, 26 January 2015; doi:10.1038/bmt.2014.315

INTRODUCTION

Allogeneic hematopoietic SCT (HSCT) has become an integral part of treatment for hematological malignancies. The risk of non-relapse mortality (NRM) after allogeneic HSCT has decreased significantly over the past few decades.[1–4] However, the risk of NRM is still high in elderly patients and patients with comorbidities.[4] Sorror *et al.*[5] established a hematopoietic cell transplantation-comorbidity index (HCT-CI) scoring system to predict the risk of NRM using pre-transplant parameters. Previous studies that assessed the impact of HCT-CI only demonstrated its impact on the overall clinical outcome.[5,6] However, detailed information about the risk of each morbidity and mortality in patients with each comorbidity is necessary so that we can intervene efficiently to reduce the risk of complications, which could be expected to improve the overall outcome.

Regarding pre-transplant diabetes mellitus (DM), Derr *et al.*[7] reported that pre-transplant hyperglycemia was associated with an increased risk of infectious diseases. However, they did not assess the impact of pre-transplant hyperglycemia on GVHD because their study mainly included patients who underwent autologous HSCT. In addition, several papers have reported that peritransplant DM was associated with an increased risk of NRM.[8–10] Our group previously showed that preengraftment hyperglycemia could be a risk factor for infectious diseases, acute GVHD and NRM.[9] However, post-transplant hyperglycemia can be caused by the post-transplant complications such as infectious diseases, which clearly increase the risk of subsequent NRM.[11,12] Therefore, the impact of pre-transplant DM on morbidity and cause-specific NRM remains unclear.

The prevalence of DM is increasing worldwide.[13–15] The number of HSCT recipients complicated with DM is also expected to increase. Thus, it is important to explore methods for improving the outcome of patients with DM in allogeneic HSCT. If we could identify morbidities which have a greater risk in patients with DM, we may be able to prevent such morbidities specifically in patients with DM in addition to glucose control, as in our previous report.[16]

In this study, we retrospectively assessed the impact of pre-transplant DM on the clinical outcome after allogeneic HSCT using the registry database of the Japan Society for Hematopoietic Cell Transplantation (JSHCT).[17]

PATIENTS AND METHODS

Patients

The clinical data were obtained from the registry database of the Transplant Registry Unified Management Program provided by the JSHCT.[17] The following patients were included in the study: (i) patients who underwent their first allogeneic HSCT between January 2007 and December 2010, and (ii) patients for whom information was available

[1]Hematopoietic Stem Cell Transplantation Division, National Cancer Center Hospital, Tokyo, Japan; [2]Department of Medical Oncology and Hematology, Oita University Faculty of Medicine, Oita, Japan; [3]Department of Hematology, Toranomon Hospital, Tokyo, Japan; [4]Division of Hematology, Department of Internal Medicine, Hyogo College of Medicine, Hyogo, Japan; [5]Hematology Division, Tokyo Metropolitan Cancer and Infectious Diseases Center Komagome Hospital, Tokyo, Japan; [6]Department of Hematology, Hamanomachi Hospital, Fukuoka, Japan; [7]Division of Epidemiology and Prevention, Aichi Cancer Center Research Institute, Nagoya, Japan; [8]Department of Hematology Oncology, Children's Medical Center, Japanese Red Cross Nagoya First Hospital, Nagoya, Japan and [9]Department of HSCT Data Management/Biostatistics, Nagoya University Graduate School of Medicine, Nagoya, Japan. Correspondence: Dr S Fuji, Hematopoietic Stem Cell Transplantation Division, National Cancer Center Hospital, 5-1-1, Tsukiji, Chuo-Ku, Tokyo 104-0045, Japan.
E-mail: sfuji@ncc.go.jp
[10]These authors contributed equally to this work.
Received 10 September 2014; revised 1 December 2014; accepted 4 December 2014

regarding the presence or absence of pre-transplant DM included in the scoring of HCT-CI. Three patients who did not have information about the overall clinical outcome were excluded. Finally, 7626 patients were included in further analyses. Data about the control of DM and the insulin-based protocols were not available owing to the nature of our registry data. This study was approved by the Institutional Review Board of National Cancer Center, Tokyo, Japan.

Clinical outcomes

Endpoints included OS, PFS, relapse/progression, NRM, infectious diseases and acute GVHD. Acute and chronic GVHD were defined based on the standard criteria.[18,19] Regarding cause-specific NRM, NRM was categorized according to the major cause of death including infection, GVHD, organ failure and other.

Statistical analysis

A descriptive statistical analysis was performed to assess the patients' characteristics. Medians and ranges are provided for continuous variables and percentages are given for categorical variables. The probabilities of OS and PFS were calculated by the Kaplan–Meier method. A Cox proportional-hazards regression model was used to analyze OS and PFS. The cumulative incidences of engraftment, NRM, GVHD and infections were evaluated using the Fine and Gray model for univariate and multivariate analyses of cumulative incidence. In the competing risk models for engraftment, GVHD and infectious disease, relapse and death before these events were defined as competing risks. In the competing risk models for NRM, relapse was defined as a competing risk. For each cause-specific NRM, relapse and NRM with other causes were defined as competing risks. Factors that were associated with a two-sided *P*-value of <0.10 in the univariate analysis were included in a multivariate analysis. We used a backward-stepwise selection algorithm and retained only the statistically significant variables in the final model. A two-sided *P*-value of <0.05 was considered statistically significant. The variables that were evaluated in these analyses were as follows: sex mismatch (female to male vs other), patient's age at the time of HSCT (age $\geqslant 40$ years vs age <40), disease risk (standard risk vs high risk), stem cell source (BM vs PB stem cells vs cord blood), HLA disparity assessed by serological typing of HLA A, B and DRB1, performance status (0–1 vs 2–4), intensity of the conditioning regimen (myeloablative conditioning vs reduced-intensity conditioning) and ABO mismatch (match vs minor mismatch vs major mismatch/major and minor mismatch). Standard risk was defined as the first CR of acute leukemia or the first chronic phase of CML or non-malignant diseases. High risk was defined as other diseases. The intensity of the conditioning regimen was defined as described previously.[20,21]

All statistical analyzes were performed with EZR (Saitama Medical Center, Jichi Medical University), which is a graphical user interface for R (The R Foundation for Statistical Computing, version 2.13.0, Dr Yoshinobu Kanda, Saitama, Japan).[22] More precisely, it is a modified version of R commander (version 1.6–3, Dr Yoshinobu Kanda) that was designed to add statistical functions that are frequently used in biostatistics.

Table 1. Patients' characteristics

	DM (n = *378*) n *(%)*	*Non-DM* (n = *7248*) n *(%)*	P-*value*
Age median (range)	58 (6–73)	43 (0–88)	<0.01
Sex combination			
Female to male	92 (24)	1599 (22)	0.21
Others	249 (66)	5046 (70)	
Missing	37 (10)	608 (8)	
Disease risk			
Standard	115 (30)	2811 (39)	<0.01
High	263 (70)	4437 (61)	
PS			
0–1	319 (84)	6083 (84)	0.26
2–4	32 (9)	763 (11)	
Missing	27 (7)	402 (5)	
Conditioning			
MAC	158 (42)	4480 (62)	<0.01
RIC	211 (56)	2669 (37)	
Missing	9 (2)	99 (1)	
Stem cell source			
Related BM	43 (11)	1261 (17)	<0.01
Related PBSC	53 (14)	1247 (17)	
Unrelated BM	184 (49)	2858 (39)	
CB	98 (26)	1882 (26)	
GVHD prophylaxis			
Cs based	125 (34)	3026 (42)	<0.01
Tacrolimus based	249 (66)	4189 (58)	
HCT-CI score			
0	0 (0)	4978 (69)	<0.01
1–2	259 (69)	1476 (20)	
$\geqslant 3$	119 (31)	784 (11)	
HCT-CI score except DM score			
0	175 (46)	4978 (69)	<0.01
1–2	129 (34)	1476 (20)	
$\geqslant 3$	74 (20)	784 (11)	

Abbreviations: CB = cord blood; DM = diabetes mellitus; HCT-CI = hematopoietic cell transplantation-comorbidity index; MAC = myeloablative conditioning; PBSC = PB stem cell; PS = performance status; RIC = reduced-intensity conditioning.

RESULTS

Patients' characteristics

Table 1 summarizes the patients' characteristics. Among the 7626 patients, 378 (5%) had pre-transplant DM (the DM group). Compared with patients without pre-transplant DM (the non-DM group), the DM group included significantly older patients, more patients with high-risk disease, more patients who received a reduced-intensity conditioning regimen and more patients who received tacrolimus.

In the DM group, 259 (69%) and 119 patients (31%) were classified as HCT-CI score = 1–2 and $\geqslant 3$, respectively. On the other hand, in the non-DM group, 1476 (20%) and 784 patients (11%) were classified as HCT-CI score = 1–2 and $\geqslant 3$, respectively. We also calculated the HCT-CI score without including the DM score to independently assess the impact of DM. When we excluded the DM score, more patients in the DM group were classified as HCT-CI score $\geqslant 1$ and this proportion was higher than that in the non-DM group (54 vs 32%, $P<0.01$). Supplementary Table 1 shows a detailed analysis of the comorbidities other than DM in each group. Patients in the DM group were more likely to be complicated by arrhythmia, cerebrovascular disease, cardiac disease, mild hepatic disease, psychiatric disturbance, obesity and prior solid tumor than those in the non-DM group.

Infections

The cumulative incidence of all documented infections at 1 year after HSCT in the DM group was significantly higher than in the non-DM group (61.5 vs 52.3%, $P<0.01$, Figure 1a). However, in a multivariate analysis, pre-transplant DM was not associated with an increased risk of documented infections. The cumulative incidence of fungal infection at 1 year after HSCT in the DM group was significantly higher than that in the non-DM group (14.9 vs 10.0%, $P=0.02$, Figure 1b). When we focused on the species of fungal infection, there was no significant difference in the cumulative incidence of aspergillus or candida infection between the two groups. Meanwhile, the cumulative incidence of mucor infection at 1 year in the DM group was significantly higher than that in the non-DM group (1.1 vs 0.1%; $P<0.01$). In a multivariate analysis, pre-transplant DM was significantly associated with an

increased risk of mucor infection (hazard ratio (HR) 9.91, 95% confidence interval (CI) 2.99–32.88, $P < 0.01$). There were no significant differences in the cumulative incidences of bacterial and viral infections at 1 year after HSCT between the groups.

Acute GVHD

There was no difference in the cumulative incidence of grade II-IV acute GVHD between the two groups (34.7 vs 34.5%, $P = 0.79$). There was also no significant difference in the cumulative incidence of grade III-IV acute GVHD between the groups (10.6 vs 11.8%, $P = 0.48$). Pre-transplant DM was not a risk factor for acute GVHD in multivariate analyses.

NRM

The median follow-up period of survivors was 583 days (range, 24–1712 days) after HSCT. Patients in the DM group had a significantly higher incidence of 1-year NRM than those in the non-DM group (36.9% vs 20.1%, $P < 0.01$, Figure 2a). In a

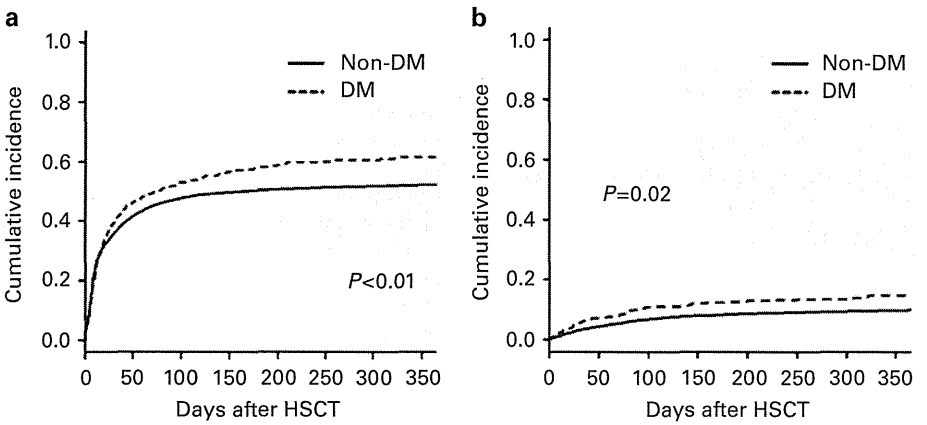

Figure 1. Cumulative incidence curves of all documented infection (**a**) and fungal infection (**b**) grouped according to the presence of pre-transplant DM.

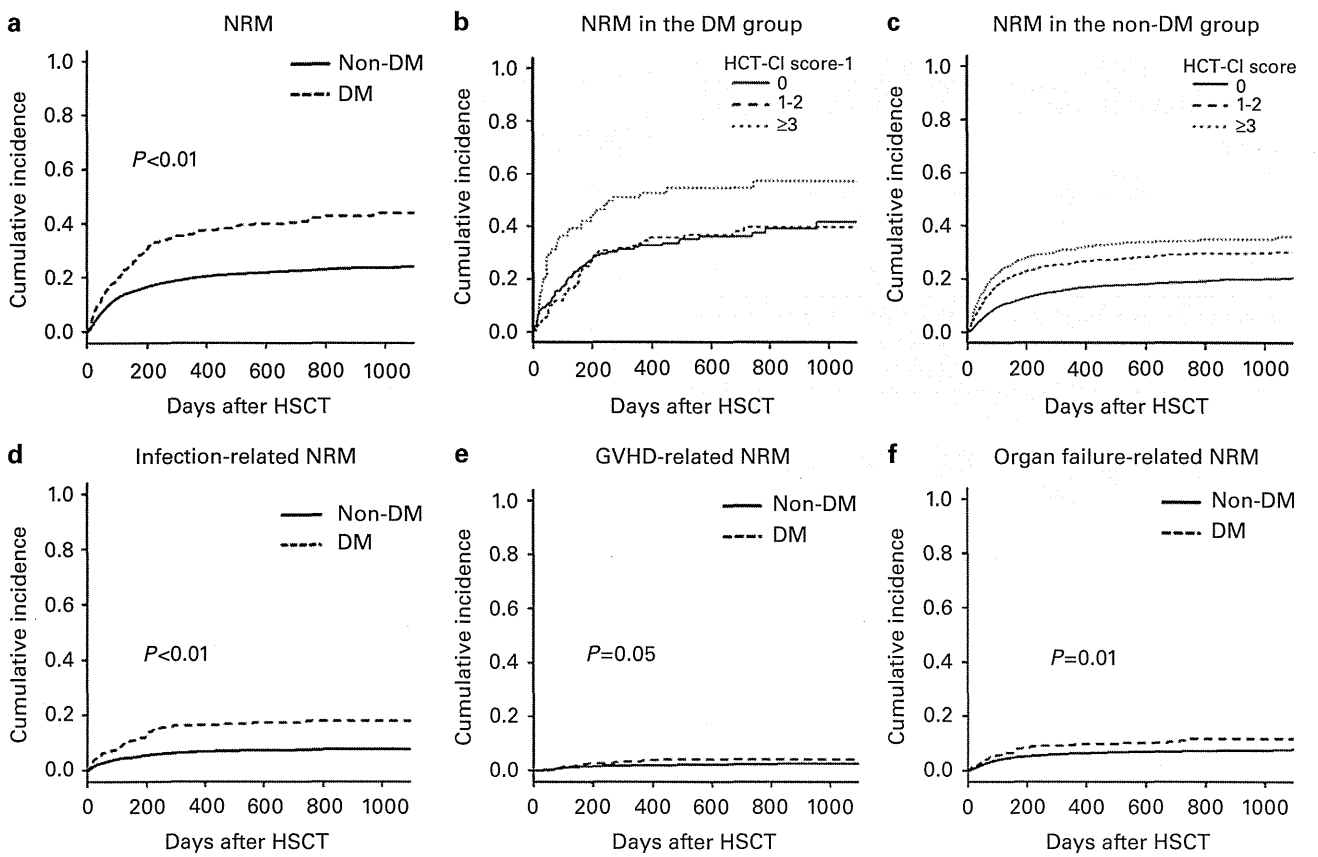

Figure 2. Cumulative incidence curves of NRM (**a**), infection-related NRM (**d**), GVHD-related NRM (**e**) and organ failure-related NRM (**f**) grouped according to the presence of pre-transplant DM. Cumulative incidence curves of NRM in the DM group stratified according to HCT-CI excluding the DM score (**b**), and in the non-DM group stratified according to the HCT-CI score (**c**).

multivariate analysis, pre-transplant DM was significantly associated with an increased risk of NRM (HR 1.46; 95% CI 1.21–1.76; $P < 0.01$, Table 2).

To exclude the impact of other comorbidities, we calculated the HCT-CI score by excluding the DM score and classified patients into three groups: score = 0, 1–2, ⩾3 in the DM group (Figure 2b) and the non-DM group (Figure 2c). The cumulative incidence of NRM at 1 year after HSCT in the DM group was significantly higher than that in the non-DM group for each HCT-CI score group. In the DM group, even in patients without any other comorbidities, the cumulative incidence of NRM at 1 year was 35% (Figure 2b). With respect to the group with score ⩾3, the cumulative incidence of NRM at 1 year increased to 52.6%, which was significantly higher than that in the non-DM group (Figures 2b and c). To further confirm the impact of DM, whilst adjusting for the impact of other HCT-CI factors, we performed a multivariate analysis of NRM that included all of the factors of HCT-CI, and pre-transplant DM was still an independent risk factor for NRM (HR 1.66; 95% CI 1.40–1.97; $P < 0.01$).

Table 2. Multivariate analysis of NRM

Covariates	*Univariate analysis*			*Multivariate analysis*		
	HR	*95% CI*	P-*value*	*HR*	*95% CI*	P-*value*
DM						
No	1.00			1.00		
Yes	2.02	1.71–2.38	< 0.01	1.46	1.21–1.76	< 0.01
Age, years						
< 40	1.00			1.00		
⩾40	2.24	1.92–2.62	< 0.01	1.96	1.66–2.31	< 0.01
Sex combination						
Female to male	1.03	0.92–1.16	0.61			
Others	1.00					
PS						
0–1	1.00			1.00		
2–4	2.41	2.13–2.73	< 0.01	2.18	1.91–2.49	< 0.01
Disease risk						
Standard	1.00			1.00		
High	1.79	1.61–1.99	< 0.01	1.39	1.25–1.56	< 0.01
Stem cell source						
Related BM	1.00			1.00		
Related PBSC	1.65	1.37–1.99	< 0.01	1.17	0.96–1.42	0.01
Unrelated BM	1.77	1.51–2.09	< 0.01	1.53	1.29–1.81	< 0.01
CB	2.52	2.13–2.98	< 0.01	1.41	1.15–1.73	< 0.01
HLA disparity						
Ag match	1.00			1.00		
1 Ag mismatch	1.55	1.37–1.76	< 0.01	1.50	1.30–1.72	< 0.01
⩾2 Ag mismatch	2.01	1.80–2.25	< 0.01	1.72	1.45–2.04	< 0.01
Conditioning						
MAC	1.00			1.00		
RIC	1.45	1.32–1.60	< 0.01	1.19	1.08–1.32	< 0.01
GVHD prophylaxis						
Cs based	1.00					
Tacrolimus based	1.24	1.13–1.37	< 0.01			

Abbreviations: CB = cord blood; CI = confidence interval; DM = diabetes mellitus; HR = hazard ratio; MAC = myeloablative conditioning; PBSC = PB stem cell; PS = performance status; RIC = reduced-intensity conditioning.

Cause-specific NRM

The cumulative incidence of infection-related NRM at 1 year after HSCT in the DM group was significantly higher than that in the non-DM group (16.4 vs 6.7%, $P < 0.01$, Figure 2d). In a multivariate analysis, pre-transplant DM was associated with an increased risk of infection-related NRM (HR 2.08, 95%CI 1.58–2.73, $P < 0.01$, Supplementary Table 2). When patients were stratified into three groups according to the pathogen of infection-related NRM (bacterial, fungal and viral), the incidence of each pathogen-related NRM was significantly higher in the DM group. Multivariate analyses showed that pre-transplant DM was associated with an increased risk of each pathogen-related NRM (bacterial, HR 1.53, 95%CI 1.01–2.32, $P = 0.04$; viral, HR 2.66, 95%CI 1.37–5.17, $P < 0.01$; fungal, HR 3.51, 95%CI 2.05–6.03, $P < 0.01$, respectively).

There was no significant difference in the cumulative incidence of GVHD-related NRM between the two groups (3.6 vs 2.0% at 1 year, $P = 0.05$, Figure 2e). In a multivariate analysis, pre-transplant DM was not a risk factor of GVHD-related NRM. The cumulative incidence of organ failure-related NRM at 1 year in the DM group was significantly higher than that in the non-DM group (9.8 vs 6.3%, $P = 0.01$, Figure 2f). In a multivariate analysis, pre-transplant DM was associated with an increased risk of organ failure-related NRM (HR 1.41, 95%CI 1.01–1.96, $P = 0.04$).

OS, PFS and relapse

The probability of OS at 1 year after HSCT in the DM group was significantly worse than that in the non-DM group (44.7 vs 63.9%, $P < 0.01$, Figure 3). A multivariate analysis showed that pre-transplant DM was associated with an inferior OS (HR 1.55, 95%CI 1.35–1.78, $P < 0.001$, Table 3). The probability of PFS at 1 year in the DM group was also significantly worse than in the

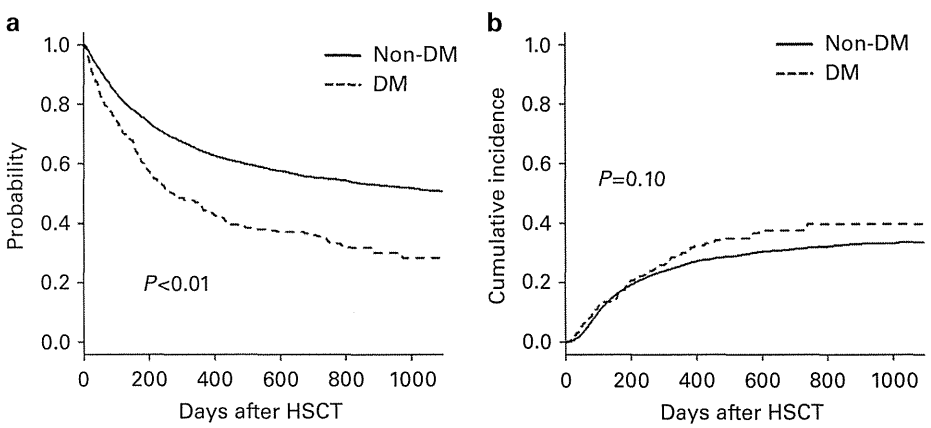

Figure 3. OS grouped according to the presence of pre-transplant DM (**a**) and cumulative incidence curves of relapse (**b**) grouped according to the presence of pre-transplant DM.

Table 3. Multivariate analysis of OS

Covariates	*Univariate analysis*			*Multivariate analysis*		
	HR	*95% CI*	*P-value*	*HR*	*95% CI*	*P-value*
DM						
No	1.00			1.00		
Yes	1.80	1.57–2.05	<.001	1.55	1.35–1.78	<0.01
Age, years						
<40	1.00			1.00		
⩾40	1.86	1.68–2.06	<0.01	1.58	1.42–1.76	<0.01
Sex combination						
Female to male	1.02	0.94–1.11	0.69			
Others	1.00					
PS						
0–1	1.00			1.00		
2–4	2.84	2.60–3.10	<0.01	2.53	2.31–2.77	<0.01
Disease risk						
Standard	1.00			1.00		
High	2.66	2.45–2.89	<0.01	2.24	2.06–2.44	<0.01
Stem cell source						
Related BM	1.00			1.00		
Related PBSC	1.67	1.47–1.89	<0.01	1.18	1.04–1.35	0.01
Unrelated BM	1.39	1.25–1.55	<0.01	1.20	1.07–1.35	<0.01
CB	2.07	1.85–2.32	<0.01	1.24	1.08–1.42	<0.01
HLA disparity						
Ag match	1.00			1.00		
1 Ag mismatch	1.37	1.25–1.50	<0.01	1.28	1.16–1.42	<0.01
⩾2 Ag mismatch	1.87	1.72–2.03	<0.01	1.49	1.33–1.67	<0.01
Intensity of conditiong						
MAC	1.00			1.00		
RIC	1.32	1.23–1.42	<0.01	1.10	1.03–1.18	0.01
GVHD prophylaxis						
Cs based	1.00					
Tacrolimus based	1.17	1.09–1.25	<0.01			

Abbreviations: CB = cord blood; CI = confidence interval; DM = diabetes mellitus; HR = hazard ratio; MAC = myeloablative conditioning; PBSC = PB stem cell; PS = performance status; RIC = reduced-intensity conditioning.

non-DM group (40.6 vs 57.4%, $P < 0.01$). In a multivariate analysis, pre-transplant DM was associated with an inferior PFS (HR 1.44, 95%CI 1.26–1.65, $P < 0.01$). Regarding relapse, there was no significant difference in the relapse rate between the two groups (30.1 vs 26.2% at 1 year, $P = 0.10$). Pre-transplant DM was not associated with an increased risk of relapse in a multivariate analysis.

DISCUSSION

In this study, we clearly demonstrated that pre-transplant DM was associated with an increased risk of NRM that led to an inferior OS. These results were consistent with previous reports by Sorror *et al.*[5,6] The estimated HR for NRM in a multivariate analysis that included all other HCT-CI factors was 1.66, which was similar to the estimated HR (HR 1.6) reported by Sorror *et al.*[6] Our study confirmed the importance of pre-transplant DM as a risk factor of NRM in allogeneic HSCT.

This study is the first to demonstrate that pre-transplant DM is associated with an increased risk of infection-related deaths. The impact of pre-transplant hyperglycemia on the risk of infection during neutropenia has been discussed previously.[7] Derr *et al.*[7] reported that pre-transplant hyperglycemia was associated with an increased risk of post-transplant infectious diseases. Even though pre-transplant DM was not a risk factor of infectious diseases in a multivariate analysis in the current study, the incidence of infection-related NRM was significantly higher in patients with DM. This might reflect the vulnerability of patients with DM to infectious diseases. In particular, in terms of fungal disease, pre-transplant DM was associated with a highly increased risk of death (HR 3.51, 95%CI 2.05–6.03, $P < 0.01$). Therefore, it might be beneficial to intensify the monitoring or the prophylaxis of fungal diseases in patients with DM. In addition, even though the overall incidence was low, the increased risk of mucor infection in patients with DM was significantly higher than in patients without DM (HR 9.91, 95% CI 2.99–32.88, $P < 0.01$), which was consistent with previous observational studies.[23,24] This finding suggests that, when patients with DM develop pneumonia that is suspected to involve *Aspergillus* or *Mucor*, it might be preferable to use antifungal agents that are active against *Mucor*, such as liposomal amphotericin B.

We also analyzed the relationship between pre-transplant DM and other factors of HCT-CI. Patients in the DM group were more likely to be complicated by arrhythmia, cerebrovascular disease, cardiac disease, mild hepatic disease, psychiatric disturbance, obesity and prior solid tumor than those in the non-DM group. This finding was consistent with previous reports.[25–30] However, pre-transplant DM was an independent risk factor of NRM in a multivariate analysis that included all other HCT-CI factors. Furthermore, when patients were stratified according to the HCT-CI score that did not include DM, the incidence of NRM in patients with DM was higher than that in those without DM. In patients with an HCT-CI score of 0, NRM at 1 year in the DM group was two times higher than that in the non-DM group (32.8 vs 16.5%, Figures 2b and c). With respect to patients with an HCT-CI score of 3 or more, 1-year NRM increased to over 52.6%. Thus, these results suggested that pre-transplant DM was associated with a poor clinical outcome independent of such coexisting comorbidities.

One possible intervention for improving the outcome could be intensive glucose control (IGC) after allogeneic HSCT. As reported previously, post-transplant hyperglycemia was common even in patients without pre-transplant DM.[8–10] Previous reports have shown that hyperglycemia is significantly associated with an increased risk of organ dysfunction, grade II–IV acute GVHD and NRM.[8–10] Therefore, we could assume that glucose control is more important in patients with pre-transplant DM. Our group recently published the results of an IGC protocol, and patients with the IGC protocol had a lower incidence of infectious diseases than a matched control cohort without IGC.[16] Even though most patients in that study did not have pre-transplant DM, IGC may offer similar benefits in patients with DM. The benefits of IGC in allogeneic HSCT for patients with DM should be assessed in future trials.

The limitations of this study should be clarified. Although this is the largest study to assess the impact of pre-transplant DM on the clinical outcome after allogeneic HSCT, as it was a retrospective analysis, we were not able to exclude the presence of uncontrolled confounding variables, even if we conducted multivariate analyzes for each clinical outcome. Thus, the present findings should be reevaluated using a different database to reconfirm the importance of pre-transplant DM. Furthermore, the data about the control of DM including the insulin-based protocols used for glycemic control should be also collected in future trials. In addition, even if pre-transplant DM was associated with an increased risk of NRM, this does not necessarily mean that intervention to normalize glucose control, so-called IGC, will

improve the outcome, as demonstrated in the field of intensive care.[31,32] The value of such interventions should be clarified in prospective studies in patients who undergo allogeneic HSCT.

In conclusion, pre-transplant DM was a significant and independent risk factor for NRM, especially infection-related deaths. To further improve the clinical outcome in patients with DM, the benefits of strict infection control and appropriate glycemic control in allogeneic HCT should be explored in future trials.

CONFLICT OF INTEREST

The authors declare no conflict of interest.

ACKNOWLEDGEMENTS

This work was supported by grants from the Japanese Ministry of Health, Labor and Welfare and the National Cancer Research and Development Fund. Some of the results were presented at the 32nd Annual Meeting of the Japanese Society of Hematology in Kanazawa, 9 March 2013. We thank the medical, nursing, data-processing, laboratory and clinical staff at the participating centers for their important contributions to this study and their dedicated care of the patients.

AUTHOR CONTRIBUTIONS

KT participated in research design, data analysis and writing of the paper; SF participated in research design, data analysis and writing of the paper; NU, HO, KO, TE, HS, YM, KK and RS gathered the data; TF participated in research design and writing of the paper. All of the authors approved the submission of this study.

REFERENCES

1 Kurosawa S, Yakushijin K, Yamaguchi T, Atsuta Y, Nagamura-Inoue T, Akiyama H *et al.* Recent decrease in non-relapse mortality due to GVHD and infection after allogeneic hematopoietic cell transplantation in non-remission acute leukemia. *Bone Marrow Transplant* 2013; **48**: 1198–1204.
2 Gooley TA, Chien JW, Pergam SA, Hingorani S, Sorror ML, Boeckh M *et al.* Reduced mortality after allogeneic hematopoietic-cell transplantation. *N Engl J Med* 2010; **363**: 2091–2101.
3 Horan JT, Logan BR, Agovi-Johnson MA, Lazarus HM, Bacigalupo AA, Ballen KK *et al.* Reducing the risk for transplantation-related mortality after allogeneic hematopoietic cell transplantation: how much progress has been made? *J Clin Oncol* 2011; **29**: 805–813.
4 Kurosawa S, Yakushijin K, Yamaguchi T, Atsuta Y, Nagamura-Inoue T, Akiyama H *et al.* Changes in incidence and causes of non-relapse mortality after allogeneic hematopoietic cell transplantation in patients with acute leukemia/myelodysplastic syndrome: an analysis of the Japan transplant outcome registry. *Bone Marrow Transplant* 2013; **48**: 529–536.
5 Sorror ML, Giralt S, Sandmaier BM, De Lima M, Shahjahan M, Maloney DG *et al.* Hematopoietic cell transplantation specific comorbidity index as an outcome predictor for patients with acute myeloid leukemia in first remission: combined FHCRC and MDACC experiences. *Blood* 2007; **110**: 4606–4613.
6 Sorror ML, Maris MB, Storb R, Baron F, Sandmaier BM, Maloney DG *et al.* Hematopoietic cell transplantation (HCT)-specific comorbidity index: a new tool for risk assessment before allogeneic HCT. *Blood* 2005; **106**: 2912–2919.
7 Derr RL, Hsiao VC, Saudek CD. Antecedent hyperglycemia is associated with an increased risk of neutropenic infections during bone marrow transplantation. *Diabetes Care* 2008; **31**: 1972–1977.
8 Hammer MJ, Casper C, Gooley TA, O'Donnell PV, Boeckh M, Hirsch IB. The contribution of malglycemia to mortality among allogeneic hematopoietic cell transplant recipients. *Biol Blood Marrow Transplant* 2009; **15**: 344–351.
9 Fuji S, Kim SW, Mori S, Fukuda T, Kamiya S, Yamasaki S *et al.* Hyperglycemia during the neutropenic period is associated with a poor outcome in patients undergoing myeloablative allogeneic hematopoietic stem cell transplantation. *Transplantation* 2007; **84**: 814–820.
10 Gebremedhin E, Behrendt CE, Nakamura R, Parker P, Salehian B. Severe hyperglycemia immediately after allogeneic hematopoietic stem-cell transplantation is predictive of acute graft-versus-host disease. *Inflammation* 2013; **36**: 177–185.
11 Esposito K, Nappo F, Marfella R, Giugliano G, Giugliano F, Ciotola M *et al.* Inflammatory cytokine concentrations are acutely increased by hyperglycemia in humans: role of oxidative stress. *Circulation* 2002; **106**: 2067–2072.
12 McCowen KC, Malhotra A, Bistrian BR. Stress-induced hyperglycemia. *Crit Care Clin* 2001; **17**: 107–124.
13 Ginter E, Simko V. Type 2 diabetes mellitus, pandemic in 21st century. *Adv Exp Med Biol* 2012; **771**: 42–50.
14 Lozano R, Naghavi M, Foreman K, Lim S, Shibuya K, Aboyans V *et al.* Global and regional mortality from 235 causes of death for 20 age groups in 1990 and 2010: a systematic analysis for the Global Burden of Disease Study 2010. *Lancet* 2012; **380**: 2095–2128.
15 Danaei G, Finucane MM, Lu Y, Singh GM, Cowan MJ, Paciorek CJ *et al.* National, regional, and global trends in fasting plasma glucose and diabetes prevalence since 1980: systematic analysis of health examination surveys and epidemiological studies with 370 country-years and 2.7 million participants. *Lancet* 2011; **378**: 31–40.
16 Fuji S, Kim SW, Mori S, Kamiya S, Yoshimura K, Yokoyama H *et al.* Intensive glucose control after allogeneic hematopoietic stem cell transplantation: a retrospective matched-cohort study. *Bone Marrow Transplant* 2009; **44**: 105–111.
17 Atsuta Y, Suzuki R, Yoshimi A, Gondo H, Tanaka J, Hiraoka A *et al.* Unification of hematopoietic stem cell transplantation registries in Japan and establishment of the TRUMP System. *Int J Hematol* 2007; **86**: 269–274.
18 Przepiorka D, Weisdorf D, Martin P, Klingemann HG, Beatty P, Hows J *et al.* 1994 Consensus Conference on Acute GVHD Grading. *Bone Marrow Transplant* 1995; **15**: 825–828.
19 Glucksberg H, Storb R, Fefer A, Buckner CD, Neiman PE, Clift RA *et al.* Clinical manifestations of graft-versus-host disease in human recipients of marrow from HL-A-matched sibling donors. *Transplantation* 1974; **18**: 295–304.
20 Bacigalupo A, Ballen K, Rizzo D, Giralt S, Lazarus H, Ho V *et al.* Defining the intensity of conditioning regimens: working definitions. *Biol Blood Marrow Transplant* 2009; **15**: 1628–1633.
21 Giralt S, Ballen K, Rizzo D, Bacigalupo A, Horowitz M, Pasquini M *et al.* Reduced-intensity conditioning regimen workshop: defining the dose spectrum. Report of a workshop convened by the center for international blood and marrow transplant research. *Biol Blood Marrow Transplant* 2009; **15**: 367–369.
22 Kanda Y. Investigation of the freely available easy-to-use software 'EZR' for medical statistics. *Bone Marrow Transplant* 2013; **48**: 452–458.
23 Rammaert B, Lanternier F, Poirée S, Kania R, Lortholary O. Diabetes and mucormycosis: a complex interplay. *Diabetes Metab* 2012; **38**: 193–204.
24 Roden MM, Zaoutis TE, Buchanan WL, Knudsen TA, Sarkisova TA, Schaufele RL *et al.* Epidemiology and outcome of zygomycosis: a review of 929 reported cases. *Clin Infect Dis* 2005; **41**: 634–653.
25 Sluik D, Boeing H, Montonen J, Pischon T, Kaaks R, Teucher B *et al.* Associations between general and abdominal adiposity and mortality in individuals with diabetes mellitus. *Am J Epidemiol* 2011; **174**: 22–34.
26 Unick JL, Beavers D, Jakicic JM, Kitabchi AE, Knowler WC, Wadden TA *et al.* Effectiveness of lifestyle interventions for individuals with severe obesity and type 2 diabetes: results from the Look AHEAD trial. *Diabetes Care* 2011; **34**: 2152–2157.
27 Mercer BN, Morais S, Cubbon RM, Kearney MT. Diabetes mellitus and the heart. *Int J Clin Pract* 2012; **66**: 640–647.
28 Shikata K, Ninomiya T, Kiyohara Y. Diabetes mellitus and cancer risk: review of the epidemiological evidence. *Cancer Sci* 2013; **104**: 9–14.
29 Eijgenraam P, Heinen MM, Verhage BA, Keulemans YC, Schouten LJ, van den Brandt PA. Diabetes type II, other medical conditions and pancreatic cancer risk: a prospective study in The Netherlands. *Br J Cancer* 2013; **109**: 2924–2932.
30 Ong JP, Younossi ZM. Epidemiology and natural history of NAFLD and NASH. *Clin Liver Dis* 2007; **11**: 1–16.
31 Inzucchi SE, Bergenstal RM, Buse JB, Diamant M, Ferrannini E, Nauck M *et al.* Management of hyperglycemia in type 2 diabetes: a patient-centered approach: position statement of the American Diabetes Association (ADA) and the European Association for the Study of Diabetes (EASD). *Diabetes Care* 2012; **35**: 1364–1379.
32 Marik PE, Preiser JC. Toward understanding tight glycemic control in the ICU: a systematic review and metaanalysis. *Chest* 2010; **137**: 544–551.

Supplementary Information accompanies this paper on Bone Marrow Transplantation website (http://www.nature.com/bmt)

Published OnlineFirst April 11, 2014; DOI: 10.1158/1078-0432.CCR-13-3169

Human Cancer Biology

Clinical Cancer Research

CADM1 Expression and Stepwise Downregulation of CD7 Are Closely Associated with Clonal Expansion of HTLV-I–Infected Cells in Adult T-cell Leukemia/Lymphoma

Seiichiro Kobayashi[1], Kazumi Nakano[5], Eri Watanabe[2], Tomohiro Ishigaki[2], Nobuhiro Ohno[3], Koichiro Yuji[3], Naoki Oyaizu[4], Satomi Asanuma[5], Makoto Yamagishi[5], Tadanori Yamochi[5], Nobukazu Watanabe[2], Arinobu Tojo[1,3], Toshiki Watanabe[5], and Kaoru Uchimaru[3]

Abstract

Purpose: Cell adhesion molecule 1 (CADM1), initially identified as a tumor suppressor gene, has recently been reported to be ectopically expressed in primary adult T-cell leukemia–lymphoma (ATL) cells. We incorporated CADM1 into flow-cytometric analysis to reveal oncogenic mechanisms in human T-cell lymphotrophic virus type I (HTLV-I) infection by purifying cells from the intermediate stages of ATL development.

Experimental Design: We isolated CADM1- and CD7-expressing peripheral blood mononuclear cells of asymptomatic carriers and ATLs using multicolor flow cytometry. Fluorescence-activated cell sorted (FACS) subpopulations were subjected to clonal expansion and gene expression analysis.

Results: HTLV-I–infected cells were efficiently enriched in $CADM1^{+}$ subpopulations (D, $CADM1^{pos}CD7^{dim}$ and N, $CADM1^{pos}CD7^{neg}$). Clonally expanding cells were detected exclusively in these subpopulations in asymptomatic carriers with high proviral load, suggesting that the appearance of D and N could be a surrogate marker of progression from asymptomatic carrier to early ATL. Further disease progression was accompanied by an increase in N with a reciprocal decrease in D, indicating clonal evolution from D to N. The gene expression profiles of D and N in asymptomatic carriers showed similarities to those of indolent ATLs, suggesting that these subpopulations represent premalignant cells. This is further supported by the molecular hallmarks of ATL, that is, drastic downregulation of miR-31 and upregulation of abnormal *Helios* transcripts.

Conclusion: The CADM1 versus CD7 plot accurately reflects disease progression in HTLV-I infection, and $CADM1^{+}$ cells with downregulated CD7 in asymptomatic carriers have common properties with those in indolent ATLs. *Clin Cancer Res; 20(11); 2851–61. ©2014 AACR.*

Introduction

Human T-cell lymphotrophic virus type I (HTLV-I) is a human retrovirus that causes HTLV-I–associated diseases, such as adult T-cell leukemia–lymphoma (ATL), HTLV-I–associated myelopathy/tropical spastic paraparesis, and HTLV-I uveitis (1–3). In Japan, the estimated lifetime risk of developing ATL in HTLV-I carriers is 6% to 7% for males and 2% to 3% for females (4–6). It takes several decades for HTLV-I–infected cells to reach the final stage of multistep oncogenesis, which is clinically recognized as aggressive ATL (acute-type and lymphoma-type; ref. 7). Molecular interaction of viral genes [e.g., Tax and the HTLV-I basic leucine zipper (HBZ) gene] with the cellular machinery causes various genetic and epigenetic alterations (7–11). However, difficulties in purifying HTLV-I–infected cells *in vivo* seem to have hindered understanding of the genetic events that are directly involved in the multistep oncogenesis of ATL.

Upregulation or aberrant expression of cell surface markers, such as CCR4 and CD25, is useful for diagnosis of ATL and has been utilized for molecular-targeted therapy (12, 13). However, the expression levels of these markers vary among patients, which often make it difficult to identify ATL cells specifically based on the immunophenotype. Previously, we focused on downregulated markers in acute-type ATL cells, such as CD3 and CD7, and successfully purified ATL cells using the CD3 versus CD7 plot of $CD4^{+}$ cells (14). Analysis of other clinical subtypes

Authors' affiliations: [1]Division of Molecular Therapy; [2]Laboratory of Diagnostic Medicine, Division of Stem Cell Therapy; [3]Department of Hematology/Oncology, Research Hospital; [4]Clinical Laboratory, Research Hospital, Institute of Medical Science; and [5]Graduate School of Frontier Sciences, The University of Tokyo, Tokyo, Japan

Note: Supplementary data for this article are available at Clinical Cancer Research Online (http://clincancerres.aacrjournals.org/).

Corresponding Author: Kaoru Uchimaru, Institute of Medical Science, The University of Tokyo, 4-6-1 Shirokanedai, Minato-ku, Tokyo 108-8639, Japan. Phone: 81-3-5449-5542; Fax: 81-3-5449-5429; E-mail: uchimaru@ims.u-tokyo.ac.jp

doi: 10.1158/1078-0432.CCR-13-3169

Published OnlineFirst April 11, 2014; DOI: 10.1158/1078-0432.CCR-13-3169

Translational Relevance

In this study, we showed that the cell adhesion molecule 1 (CAMD1) versus CD7 plot reflects the progression of disease in patients infected with human T-cell lymphotrophic virus type I (HTLV-I), in that the proportion of $CADM1^{+}$ subpopulations (D, $CADM1^{pos}CD7^{dim}$ and N, $CADM1^{pos}CD7^{neg}$) increased with the progression from HTLV-I asymptomatic carrier (AC) to indolent adult T-cell leukemia–lymphoma (ATL) to aggressive ATL. We confirmed the purity of the clonal HTLV-I–infected cells in these subpopulations of various clinical subtypes, including asymptomatic carriers. The results from the flow-cytometric analysis will help physicians assess disease status. The analysis is also practical in screening for putative high-risk HTLV-I asymptomatic carriers, which show nearly identical flow-cytometric and gene expression profiles with those of smoldering-type ATL patients. Furthermore, cell sorting by flow cytometry enables purification of clonally expanding cells in various stages of oncogenesis in the course of progression to aggressive ATL. Detailed molecular analysis of these cells will provide valuable information about the molecular events involved in multistep oncogenesis of ATL.

(indolent ATLs and HTLV-I asymptomatic carriers; AC) revealed that HTLV-I–infected and clonally expanded cells were purified similarly and that the subpopulations with downregulated CD7 grew concomitantly with the progression of HTLV-I infection (15). Although this type of flow-cytometric analysis was shown to be a useful tool, a substantial subpopulation of T cells shows downregulated expression of CD7 under physiologic (16, 17) and certain pathologic conditions, including autoimmune disorders, viral infection, and hematopoietic stem cell transplantation (18–23).

Recently, Sasaki and colleagues reported ectopic overexpression of the cell adhesion molecule 1/tumor suppressor in lung cancer 1 (CADM1/TSLC1) gene in primary acute-type ATL cells based on expression profile analysis (24, 25). CADM1 (/TSLC1) is a cell-adhesion molecule that was originally identified as a tumor suppressor in lung cancers (25, 26). In addition, numbers of $CD4^{+}$ $CADM1^{+}$ cells have been found to be significantly correlated with the proviral load (PVL) in both ATLs and HTLV-I asymptomatic carriers (25, 27). Thus, CADM1 is a good candidate marker of HTLV-I–infected cells. In the present study, we incorporated CADM1 into our flow-cytometric analysis. In the CADM1 versus CD7 plot of $CD4^{+}$ cells, HTLV-I–infected and clonally expanded cells were efficiently enriched in the $CADM1^{+}$ subpopulations regardless of disease status. In these cells, stepwise CD7 downregulation (from dimly positive to negative) occurred with disease progression. The proportion of the three subpopulations observed in this plot [P, $CADM1^{negative(neg)}CD7^{positive(pos)}$; D, $CADM1^{pos}CD7^{dim}$; and N, $CADM1^{pos}$ $CD7^{neg}$] accurately reflected the disease status in HTLV-I infection. The analysis of comprehensive gene expression in each subpopulation revealed that the expression profile of $CADM1^{+}$ subpopulations in indolent ATLs showed similarities with that in asymptomatic carriers with high PVL; yet, it was distinct from that in aggressive ATLs. These D and N subpopulations were indicative of HTLV-I–infected cells in the intermediate stage of ATL development.

Materials and Methods

Cell lines and patient samples

TL-Om1, an HTLV-I–infected cell line (28), was provided by Dr. Sugamura (Tohoku University, Sendai, Japan). The MT-2 cell line was a gift from Dr. Miyoshi (Kochi University, Kochi, Japan) and ST-1 was from Dr. Nagai (Nagasaki University, Nagasaki, Japan). Peripheral blood samples were collected from in-patients and out-patients at our hospital, as described in our previous reports (14, 15). As shown in Supplementary Table S1, 26 cases were analyzed (10 cases of asymptomatic carrier; 5 cases of smoldering-type; 6 cases of chronic-type; and 5 cases of acute-type). All patients with ATL were categorized into clinical subtypes according to Shimoyama's criteria (12, 29). Patients with various complications, such as autoimmune disorders and systemic infections, were excluded. Lymphoma-type patients were also excluded because ATL cells are not considered to exist in the peripheral blood of this clinical subtype. Samples collected from six healthy volunteers (mean age 48.8 years; range 34–66 years) were used as normal controls. The present study was approved by the Institutional Review Board of our institute (the University of Tokyo, Tokyo, Japan). Written informed consent was obtained from all patients and healthy volunteers.

Flow cytometry and cell sorting

Peripheral blood mononuclear cells (PBMC) were isolated from whole blood by density gradient centrifugation, as described previously (14). An unlabeled CADM1 antibody (clone 3E1) and an isotype control chicken immunoglobulin Y (IgY) antibody were purchased from MBL. These were biotinylated (primary amine biotinylation) using biotin N-hydroxysuccinimide ester (Sigma-Aldrich). Pacific Orange-conjugated anti-CD14 antibody was purchased from Caltag-Invitrogen. All other antibodies were obtained from BioLegend. Cells were stained using a combination of biotin-CADM1, allophycocyanin (APC)-CD7, APC-Cy7-CD3, Pacific Blue-CD4, and Pacific Orange-CD14. After washing, phycoerythrin-conjugated streptavidin was applied. Propidium iodide (Sigma-Aldrich) was added to the samples to stain dead cells immediately before flow cytometry. A FACSAria instrument (BD Immunocytometry Systems) was used for all multicolor flow cytometry and fluorescence-activated cell sorting (FACS). Data were analyzed using FlowJo software (TreeStar). The gating

Published OnlineFirst April 11, 2014; DOI: 10.1158/1078-0432.CCR-13-3169

procedure for a representative case is shown in Supplementary Fig. S1.

Quantification of HTLV-I proviral load by real-time quantitative PCR

PVL in FACS-sorted PBMCs was quantified by real-time quantitative PCR (TaqMan method) using the ABI Prism 7000 sequence detection system (Applied Biosystems), as described previously (14, 30).

Evaluation of HTLV-I *HBZ* gene amplification by semiquantitative PCR

HTLV-I *HBZ* gene amplification was performed as described previously (25). Briefly, the 25-μL PCR mixture consisted of 20 pmol of each primer, 2.0 μL of mixed deoxynucleotide triphosphates (2.5 mmol/L each), 2.5 μL of 10× PCR buffer, 1.5 μL of $MgCl_2$ (25 mmol/L), 0.1 μL of AmpliTaq Gold DNA Polymerase (Applied Biosystems), and 20 ng of DNA extracted from cell lines and clinical samples. The PCR consisted of initial denaturation at 94°C for 9 minutes, 30 cycles of 94°C for 30 seconds, 57°C for 30 seconds, and 72°C for 45 seconds, followed by 72°C for 5 minutes. The β-actin gene (*ACTB*) was used as an internal reference control. The primer sequences used were as follows: HBZ forward, 5′-CGCTGCCGATCACGATG-3′; HBZ reverse, 5′-GGAGGAATTGGTGGACG-3′; ACTB forward, 5′-CGTGCTCAGGGCTTCTT-3′; and ACTB reverse, 5′-TGAAGGTCTCAAACATGATCTG-3′. Amplification with these pairs of oligonucleotides yielded 177-bp HBZ and 731-bp β-actin fragments.

FISH for quantification of HTLV-I–infected cells

FISH analysis was performed to detect HTLV-I proviral DNA in mononuclear cells that had been FACS-sorted on the basis of the CADM1 versus CD7 plot. These samples were sent to a commercial laboratory (Chromosome Science Labo Inc.), where FISH analysis was performed. Briefly, pUC/HTLV-I plasmid containing the whole-HTLV-I genome was labeled with digoxigenin by the nick translation method, and was then used as a FISH probe. Pretreatment, hybridization, and washing were performed according to standard laboratory protocols. To remove fluorochrome-labeled antibodies attached to the cell surface, pretreatment consisted of treatment with 0.005% pepsin and 0.1 N HCl. The FISH probe was detected with Cy3-labeled anti-digoxigenin antibody. Cells were counterstained with 4′, 6 diamidino-2-phenylindole. The results were visualized using a DMRA2 conventional fluorescence microscope (Leica) and photographed using a Leica CW4000 cytogenetics workstation. Hybridization signals were evaluated in approximately 100 nuclei.

Inverse long PCR to assess the clonality of HTLV-I–infected cells

For clonality analysis, inverse long PCR was performed as described previously (14). First, 1 μg genomic DNA extracted from the FACS-sorted cells was digested with *PstI* or *Eco*RI at 37°C overnight. RNase A (Qiagen) was added to remove residual RNA completely. DNA fragments were purified using a QIAEX2 Gel Extraction Kit (Qiagen). The purified DNA was self-ligated with T4 DNA ligase (Takara Bio) at 16°C overnight. After ligation of the *Eco*RI-digested samples, the ligated DNA was further digested with *MluI*, which cuts the pX region of the HTLV-I genome and prevents amplification of the viral genome. Inverse long PCR was performed using Tks Gflex DNA Polymerase (Takara Bio). For the *PstI*-treated group, the forward primer was 5′-CAGCCCATTCTATAGCACTCTCCAGGAGAG-3′ and the reverse primer was 5′-CAGTCTCCAAACACGTAGACTGGGTATCCG-3′. For the *Eco*RI-treated template, the forward primer was 5′-TGCCTGACCCTGCTTGCTCAACTCTACGTCTTTG-3′ and the reverse primer was 5′-AGTCTGGGCCCTGACCTTTTCAGACTTCTGTTTC-3′. Processed genomic DNA (50 ng) was used as a template. The reaction mixture was subjected to 35 cycles of denaturation (94°C, 30 seconds) and annealing plus extension (68°C, 8 minutes). Following PCR, the products were subjected to electrophoresis on 0.8% agarose gels. Fourteen patient samples were analyzed. For samples from which a sufficient amount of DNA was extracted, PCR was generally performed in duplicate.

Gene expression microarray analysis of each subpopulation in the CADM1 versus CD7 plot

Total RNA was extracted from each subpopulation in the CADM1 versus CD7 plot using TRIzol (Invitrogen) according to the manufacturer's protocol. Details of the clinical samples used for microarray analyses are shown in Supplementary Table S1. Treatment with DNase I (Takara Bio) was conducted to eliminate genomic DNA contamination. The quality of the extracted RNA was assessed using a BioAnalyzer 2000 system (Agilent Technologies). The RNA was then Cy3-labeled using a Low Input Quick Amp Labeling Kit (Agilent Technologies). Labeled cRNA samples were hybridized to 44K Whole Human Genome Oligonucleotide Microarrays (Agilent Technologies) at 65°C for 17 hours. After hybridization, the microarrays were washed and scanned with a Scanner C (Agilent Technologies). Signal intensities were evaluated by Feature Extraction 10.7 software and then analyzed using Gene Spring 12.0 software (Agilent Technologies). Unsupervised two-dimensional hierarchical clustering analysis (Pearson correlation) was performed on 10,278 genes selected by one-way ANOVA ($P < 0.05$). The dataset for these DNA microarrays has been deposited in Gene Expression Omnibus (accession number GSE55851).

Expression analysis of miR-31 and *Helios* transcript variants of each subpopulation in the CADM1 versus CD7 plot

The expression levels of the microRNA miR-31 were quantified using a TaqMan-based MicroRNA Assay (Applied Biosystems), as described previously (31), and normalized to RNU48 expression level. Helios mRNA transcript variants were examined using reverse transcription

Published OnlineFirst April 11, 2014; DOI: 10.1158/1078-0432.CCR-13-3169

PCR (RT-PCR) with Platinum Taq DNA Polymerase High Fidelity (Invitrogen), as described previously (32). To detect and distinguish alternative splicing variants, PCR analyses were performed with sense and antisense primer sets specific for the first and final exons of the Helios gene. The PCR products were then sequenced to determine the exact type of transcript variant. A mixture of Hel-1, Hel-2, Hel-5, and Hel-6 cDNA fragments was used as a "Helios standard" in the electrophoresis of RT-PCR samples.

Results

CADM1 expression based on the CD3 versus CD7 plot in CD4$^+$ cells in primary HTLV-I–infected blood samples

The clinical profiles of the 32 cases analyzed are shown in Supplementary Table S1. We first examined CADM1 expression in each subpopulation (H, I, and L) of the CD3 versus CD7 plot. Representative data (for a case of smoldering ATL) are shown in Fig. 1A. The results demonstrate that

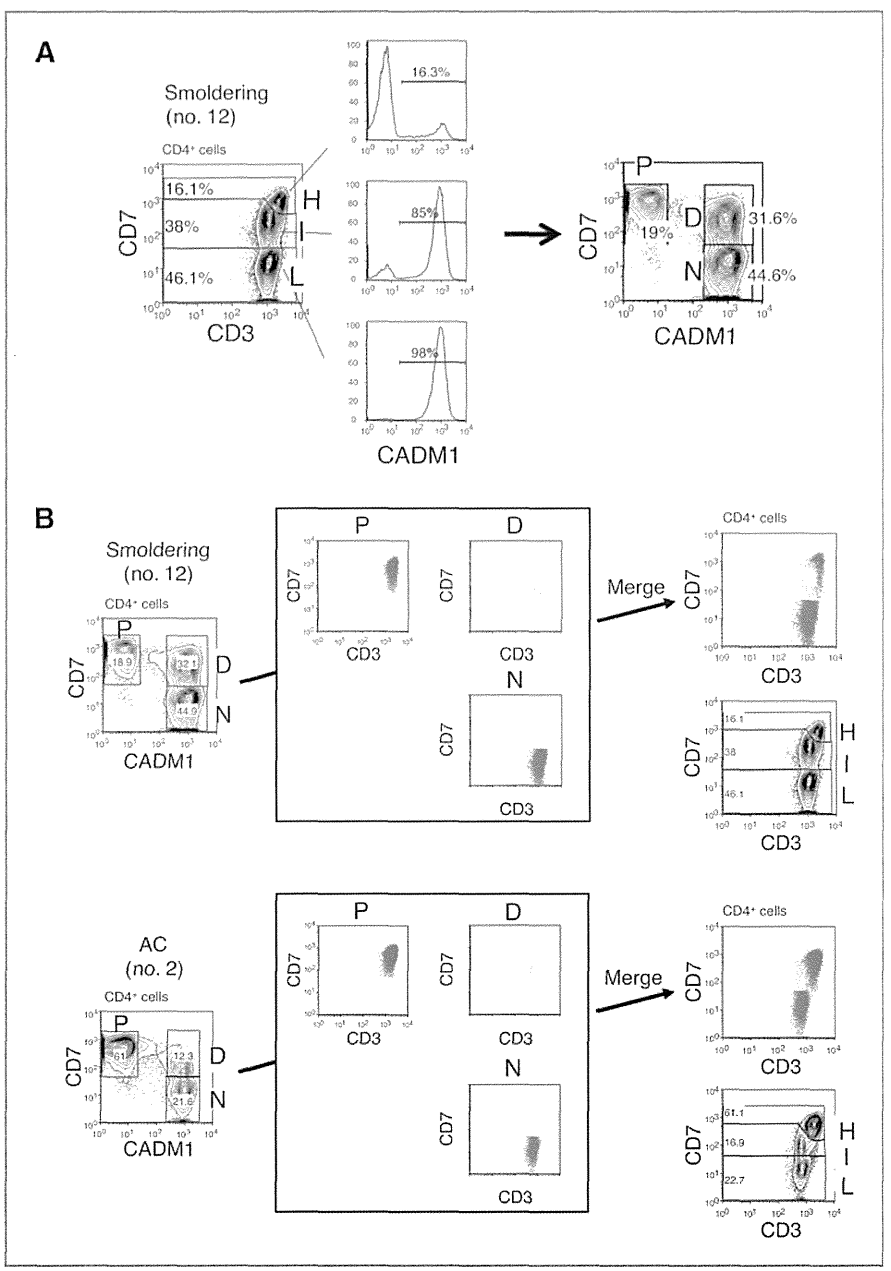

Figure 1. CADM1 versus CD7 plot for CD4$^+$ cells from HTLV-I–infected blood samples analyzed by flow cytometry. A, representative flow-cytometric analysis of a patient with smoldering-type ATL. Three subpopulations (H, I, and L) were observed in the CD3 versus CD7 plot for CD4$^+$ cells (left). Expression of CADM1 in each subpopulation is shown (middle). The right-hand panel shows how the CADM1 versus CD7 plot for CD4$^+$ cells was constructed. B, the P, D, and N subpopulations in the CADM1 versus CD7 plot correspond to the H, I, and L subpopulations in the CD3 versus CD7 plot. Blue, yellow, and red dots, respectively, indicate the P, D, and N subpopulations in the CADM1 versus CD7 plot, and are redrawn in the CD3 versus CD7 plot. Two representative cases are shown. In the upper case, the P and D subpopulations in the CADM1 versus CD7 plot are partly intermingled in the CD3 versus CD7 plot. Unlike the CD3 versus CD7 plot, the CADM1 versus CD7 plot clearly distinguishes three subpopulations.

Published OnlineFirst April 11, 2014; DOI: 10.1158/1078-0432.CCR-13-3169

CADM1 was expressed almost exclusively in the I and L subpopulations. Drawing a CADM1 versus CD7 plot for $CD4^+$ cells revealed three distinct subpopulations (P, $CADM1^{neg}CD7^{pos}$; D, $CADM1^{pos}CD7^{dim}$; and N, $CADM1^{pos}$ $CD7^{neg}$). As shown in Fig. 1B, the P, D, and N subpopulations corresponded to the H, I, and L subpopulations in the CD3 versus CD7 plot. In the previous CD3 versus CD7 plot, the lower case (AC no. 2) showed three distinct subpopulations. However, in the upper case (smoldering no. 12), the H and I subpopulations substantially intermingled with each other and were not clearly separated. In contrast, the CADM1 versus CD7 plot clearly revealed three distinct subpopulations in both cases.

HTLV-I–infected cells are highly enriched in $CADM1^+$ subpopulations

On the basis of previous reports (25, 27), we expected HTLV-I–infected cells to be enriched in the $CADM1^+$ subpopulations in our analysis. Figure 2A shows the PVL measurements of the three subpopulations in the CADM1 versus CD7 plot for three representative cases. HTLV-I–infected cells were highly enriched in the $CADM1^+$ subpopulations (D and N). The PVL data indicate that most of the cells in the D and N subpopulations were HTLV-I infected. Figure 2B shows the results of semiquantitative PCR of the *HBZ* gene in representative cases. In the D and N subpopulations, the *HBZ* gene was amplified to the same degree as in the HTLV-I–positive cell line. To confirm these results, FISH was performed in one asymptomatic carrier. As shown in Supplementary Fig. S2, HTLV-I–infected cells were highly enriched in the D and N subpopulations, which supports the results of the PVL analysis and semiquantitative PCR of the *HBZ* gene. In the FISH analysis, percentages of HTLV-I–infected cells in D and N did not reach 100%. This may have been due to a technical issue. Because the cells subjected to FISH analysis were sorted by FACS, several fluorochrome-conjugated antibodies may have remained on their surfaces, even after treatment with protease.

The CADM1 versus CD7 plot accurately reflects disease progression in HTLV-I infection

Compared with the CD3 versus CD7 plot, the CADM1 versus CD7 plot was revealed to be clear in its distinction of the three subpopulations and efficient in enrichment of HTLV-I–infected cells. On the basis of these findings, we analyzed clinical samples of asymptomatic carriers and three clinical subtypes of ATL: the smoldering, chronic, and acute subtypes. Data for representative cases, presented in Fig. 3A, suggest that the continual changes in the proportions of the three subpopulations are associated with disease progression. In the CADM1 versus CD7 plot, normal control samples showed a P-dominant pattern. With progression of the disease from the asymptomatic carrier state with a low PVL to that with a high PVL, and to indolent-type ATL, the D and N subpopulations increased gradually. As the disease further progressed to acute-type ATL, the N subpopulation showed remarkable expansion. Data for all analyzed samples are presented in Fig. 3B. The results suggest that the CADM1 versus CD7 plot of peripheral blood samples represents progression of the disease in HTLV-I carriers. Data for the normal control cases analyzed are shown in Supplementary Fig. S3. In all normal controls, the percentages of the D and N subpopulations were low. Supplementary Fig. S4 shows temporal data for a patient with chronic-type ATL who progressed from stable disease to a relatively progressive state and the concomitant change in the flow cytometry profile.

Clonality analysis of the three subpopulations in the CADM1 versus CD7 plot

To characterize the three subpopulations further, the clonal composition of each subpopulation was analyzed by inverse long PCR, which amplifies part of the provirus

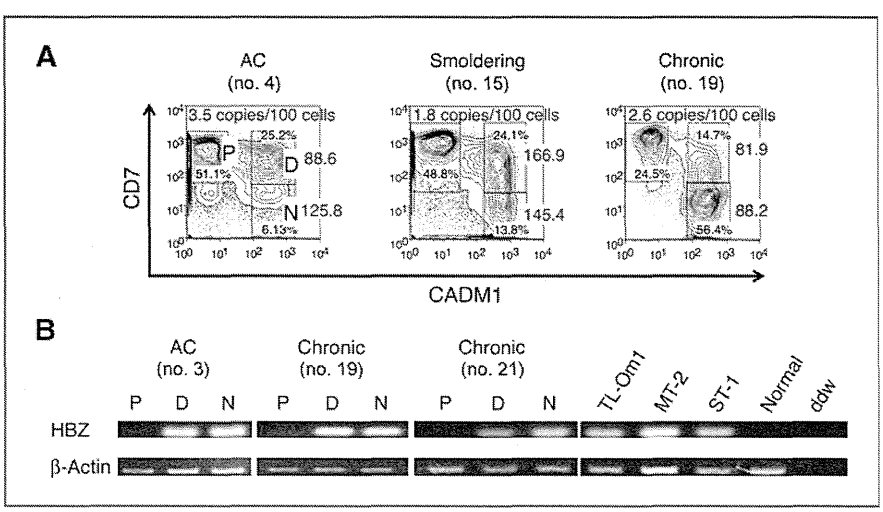

Figure 2. HTLV-I–infected cells are highly enriched in the $CADM1^+$ subpopulations. A, analysis of PVL in the three subpopulations. Three representative cases are shown. PVL data (copies/100 cells) are shown in red. Percentages of each subpopulation are shown in black. B, semiquantitative PCR of the *HBZ* gene in the three subpopulations in three representative cases. Normal, DNA from PBMCs from a normal control; ddw, deionized distilled water.

Published OnlineFirst April 11, 2014; DOI: 10.1158/1078-0432.CCR-13-3169

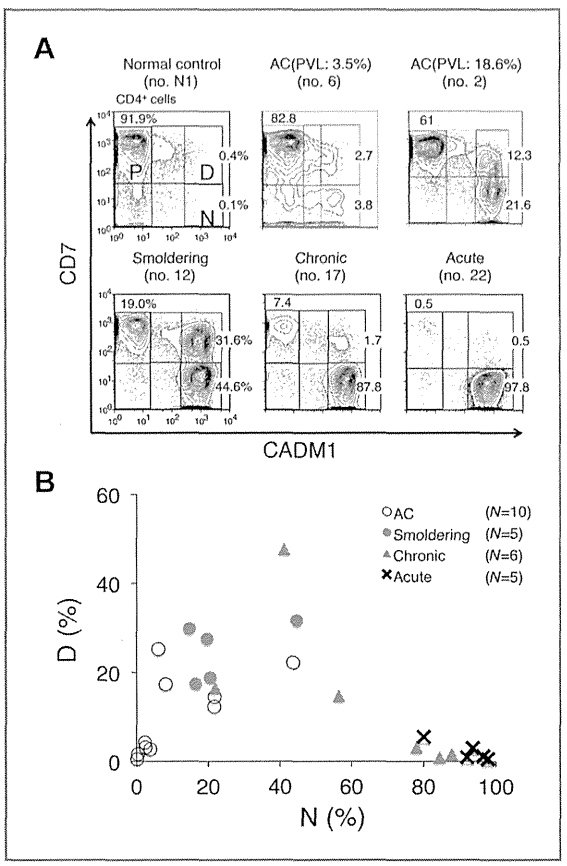

Figure 3. Proportion of each subpopulation in the CADM1 versus CD7 plots for asymptomatic HTLV-I carriers (asymptomatic carriers) and ATLs of various clinical subtypes. A, data of representative cases are shown. B, a two-dimensional plot of all analyzed samples showing the percentages of the D and N subpopulations.

long terminal repeat and the flanking genomic sequence of the integration sites. Cells in each subpopulation were sorted by FACS, and subjected to inverse long PCR analysis. Representative results for smoldering-, chronic-, and acute-type ATL samples are presented in Fig. 4A. Major clones, indicated by intense bands, were detected in the D and N subpopulations. The major clones in the D and N subpopulations in each case were considered to be the same based on the sizes of the amplified bands, suggesting that clonal evolution is accompanied by downregulation of CD7 expression. Fig. 4B shows representative results for three cases of asymptomatic carrier. In all cases, weak bands in the P subpopulation were visible, indicating that this population contains only minor clones. In these asymptomatic carriers, the proportion of abnormal lymphocytes and PVL increases from left to right. The consistent increase in the D and N subpopulations, together with growth of major clones as shown in the inverse PCR analysis, were considered to reflect these clinical data.

Gene expression profiling of the three subpopulations in the CADM1 versus CD7 plot

To determine the molecular basis for the biologic differences among the three subpopulations in the CADM1 versus CD7 plot, we next characterized the gene-expression profiles of the subpopulations of the following clinical subgroups: asymptomatic carriers ($n = 2$), smoldering-type ATLs ($n = 2$), chronic-type ATL ($n = 1$), acute-type ATLs ($n = 3$), and normal controls ($n = 3$). The two asymptomatic carriers (nos. 5 and 9) had high PVLs (11.6 and 26.2%, respectively) and relatively high proportions of D and N subpopulations (Supplementary Table S1). Unsupervised hierarchical clustering analysis of the results revealed three clusters (A, B1, and B2) or two major clusters A and B, where A is composed solely of the samples of the acute-type N subpopulation and B is subdivided into two clusters (B1 and B2; Fig. 5A). The B2 cluster is composed of the P subpopulation of all clinical subtypes and of normal controls, whereas the B1 cluster is composed of the D and N subpopulations of

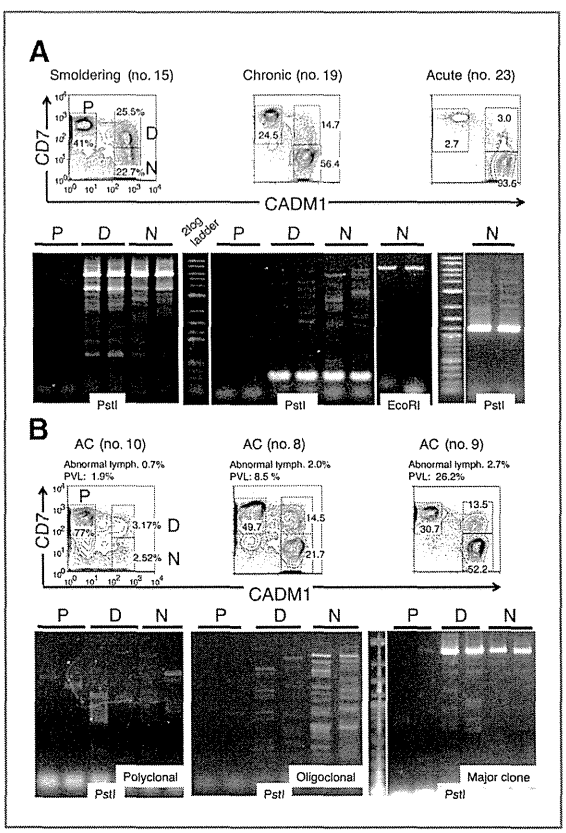

Figure 4. Clonality of subpopulations in the CADM1 versus CD7 plot analyzed by inverse long PCR. FACS-sorted cells (P, D, and N) were subjected to inverse long PCR. The black bar indicates duplicate data. Flow-cytometric profiles and clinical data are also presented. A, representative cases of smoldering-, chronic-, and acute-type ATL are shown. B, representative cases of asymptomatic carriers are shown.

Published OnlineFirst April 11, 2014; DOI: 10.1158/1078-0432.CCR-13-3169

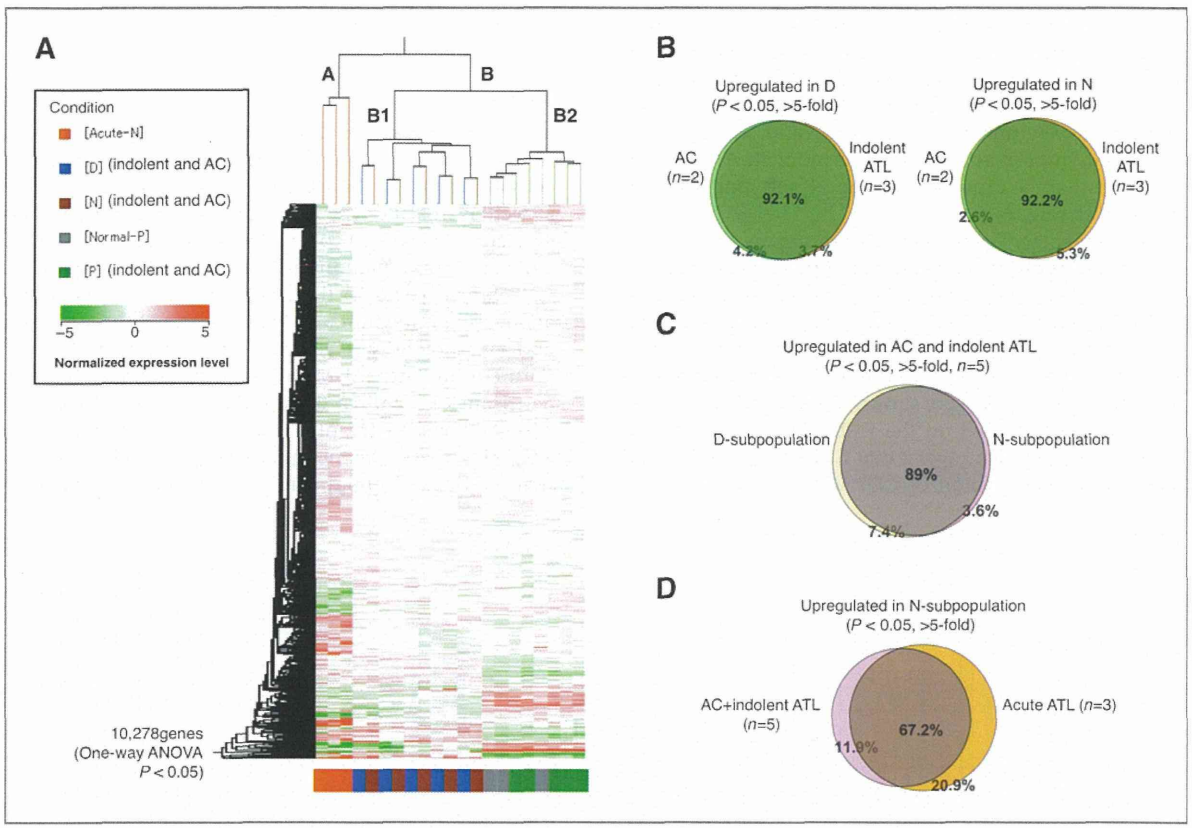

Figure 5. Comprehensive gene expression analysis of the three subpopulations in the CADM1 versus CD7 plot. A, we conducted an unsupervised hierarchical clustering analysis of 10,278 genes whose expression levels were significantly changed in the P subpopulation of normal controls ($n = 3$); P, D, and N subpopulations of asymptomatic carriers and indolent ATLs ($n = 5$); and N subpopulation of acute-ATLs ($n = 3$; one-way ANOVA, $P < 0.05$). The P and D subpopulations of acute ATLs and D and N subpopulations of normal controls could not be analyzed because of insufficient numbers of cells. Clustering resulted in three major clusters: (i) P subpopulations of normal controls (gray) and asymptomatic carriers/indolent ATLs (green); (ii) D and N subpopulations of asymptomatic carriers/indolent ATLs (blue and brown, respectively); and (iii) N subpopulations of acute ATLs (red). These results indicate that the P subpopulations of asymptomatic carriers/indolent ATLs have characteristics similar to those of normal uninfected cells, whereas the D and N subpopulations of asymptomatic carriers/indolent ATLs have genetic lesions in common. The N subpopulations of acute ATLs are grouped in an independent cluster, meaning that these malignant cell populations have a significantly different gene expression profile, even compared with the N subpopulations of indolent ATLs. B, similarity between asymptomatic carriers and indolent ATLs. The Venn diagrams show that 92.1% and 92.2% of genes upregulated in the D and N subpopulations, respectively, compared with "Normal-P" ($P < 0.05$), were common to asymptomatic carriers ($n = 2$) and indolent ATLs ($n = 3$). C, similarity between the D and N subpopulations. The Venn diagram shows that 89% of genes upregulated in the D and N subpopulation, compared with Normal-P ($P < 0.05$), overlapped. D, comparison of the N subgroups between acute-ATLs ($n = 3$) and asymptomatic carriers/indolent ATLs ($n = 5$). As shown in the Venn diagram, 67.2% of genes were upregulated ($P < 0.05$) in the N subpopulations of both acute ATLs and asymptomatic carrier/indolent ATLs. However, a significant number of genes (20.9%) were upregulated only in the N subpopulation of acute ATLs.

asymptomatic carriers and indolent ATLs (smoldering- and chronic-type).

Figure 5B shows a Venn diagram of the upregulated genes in the D subpopulation (left) or the N subpopulation (right) common to asymptomatic carriers ($n = 2$) and indolent ATLs ($n = 3$). These diagrams demonstrate that the changes in the gene expression profiles of the D and N subpopulations of asymptomatic carriers were similar to those of indolent ATLs. Furthermore, the gene expression profiles of the D and N subpopulations of asymptomatic carriers and indolent ATLs were similar (Fig. 5C). In contrast, the upregulated genes showed distinct differences between the N subpopulation of acute-type ATL and that of indolent ATLs and asymptomatic carriers, although approximately 70% were common to both (Fig. 5D).

Expression of a tumor suppressor microRNA and splicing abnormalities of Ikaros family genes in the three subpopulations

To determine whether the novel subpopulations identified had other properties in common with ATL cells, we examined miR-31 levels and *Helios* mRNA patterns in sorted subpopulations (31, 32). Expression of miR-31 decreased drastically in the D subpopulation derived from indolent ATLs and asymptomatic carriers, and was

Published OnlineFirst April 11, 2014; DOI: 10.1158/1078-0432.CCR-13-3169

even lower in the N subpopulation derived from asymptomatic carriers and indolent/acute ATLs (Fig. 6A). In addition, examination of *Helios* mRNA transcript variants revealed that expression levels of *Hel-2*, which lacks part of exon 3, were upregulated in the D and N subpopulations of asymptomatic carriers and indolent ATLs, and it was dominantly expressed in the N subpopulation of acute ATLs (Fig. 6B).

Supplementary Fig. S5 presents a summary of this study. The representative flow-cytometric profile shows how the CADM1 versus CD7 plot reflects disease progression in HTLV-I infection. The plot together with the gene expression profiles clearly distinguished the subpopulations of distinct oncogenic stages. The groups classified according to gene expression profile are shown as blue, yellow, and red and are superimposed on the CADM1 versus CD7 plot. Collectively, our data suggest that CADM1 expression and stepwise downregulation of CD7 were closely associated with clonal expansion of HTLV-I–infected cells in ATL progression.

Discussion

We showed that the CADM1 versus CD7 plot is capable of discriminating clonally expanding HTLV-I–infected cells in indolent ATLs and even in asymptomatic carriers, as well as in acute-type ATLs. Our analysis demonstrated efficient enrichment of HTLV-I–infected cells in the $CADM^+$ subpopulations (D and N in the CADM1 vs. CD7 plot), based on the results of real-time PCR (PVL analysis), semiquantitative PCR analysis of the *HBZ* gene, and FISH analysis (Fig. 2 and Supplementary Fig. S2). Furthermore, the CADM1 versus CD7 plot was shown to discriminate the three subpopulations more clearly than the CD3 versus CD7 plot (Fig. 1). Clonality analysis of ATLs and asymptomatic carriers (Fig. 4A and B) revealed that $CADM1^+$ subpopulations (D and N) contained

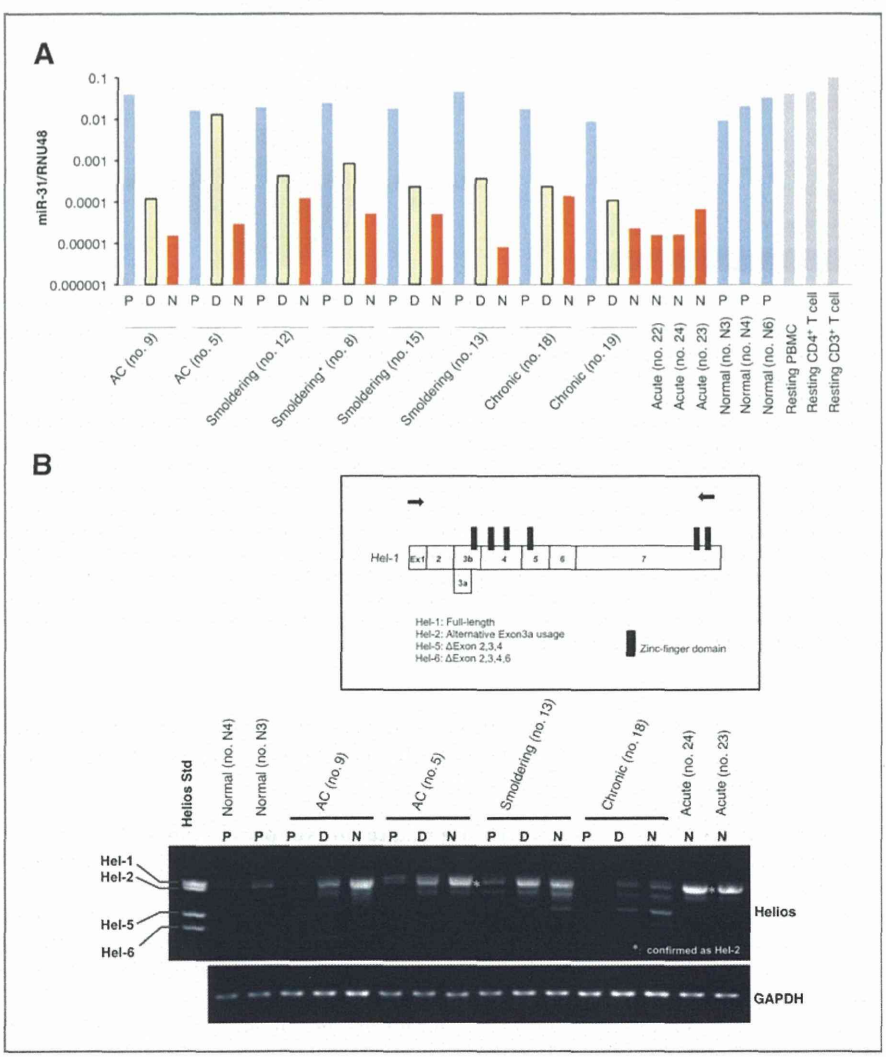

Figure 6. Gene expression pattern in the CADM1/CD7 subpopulation. A, miR-31 expression levels quantified by TaqMan-based real-time PCR. Total RNAs derived from each subpopulation were isolated and analyzed by RT-real-time PCR. RNU48 levels were also measured as an internal normalizer. *Smoldering (no. 8), this patient was considered to be at the asymptomatic carrier/smoldering borderline, because the proportion of abnormal lymphocytes fluctuated around 5%. On the day of sampling, the patient's hemogram showed 6.5% abnormal lymphocytes. B, expression analysis of *Helios* transcript variants in the subpopulations of normal controls ($n = 2$), asymptomatic carriers ($n = 2$), and ATLs (smoldering-type ATL, $n = 1$; chronic-type ATL, $n = 1$; acute-type ATL, $n = 2$). Comparisons of transcript variants among the P, D, and N subpopulations were performed by RT-PCR using primer sets specific for full-length *Helios* cDNA (top). The primer locations for *Helios* PCR are indicated by arrows in the schematic representation of *Hel-1*. The amplified cDNA (asterisk) was confirmed to be the *Hel-2* variant. The *Helios* standard (left lane), a mixture of cDNA fragments of *Hel-1*, *Hel-2*, *Hel-5*, and *Hel-6*, was used as a size indicator for each transcript variant. The glyceraldehyde-3-phosphate dehydrogenase (*gapdh*) mRNA was analyzed as an internal control (bottom).

Published OnlineFirst April 11, 2014; DOI: 10.1158/1078-0432.CCR-13-3169

clonally expanded HTLV-I–infected cells, whereas cells in the P subpopulation ($CADM1^-$) did not show clonal expansion in this analysis. Current molecular analyses of ATL cells have been limited to HTLV-I–infected cell lines and primary cells from acute/lymphoma type ATL, because in these cases, the predominant expanding clones are readily available with relatively high purity. However, the separation of clonally expanding ATL cells from indolent ATLs and asymptomatic carriers has not yet been achieved. The CADM1 versus CD7 plot from FACS allows efficient purification of such clones *in vitro*.

In an unsupervised clustering analysis of the gene expression data, the D and N subpopulations of asymptomatic carriers/indolent ATLs were grouped together, suggesting that the biologic characteristics of these subpopulations are similar (Fig. 5A and B) but distinct from the N subpopulation of acute-type ATLs (Fig. 5D). These results support the notion that in indolent ATLs and even in asymptomatic carriers, the D and N subpopulations are clonally expanding cells representing the intermediate oncogenic stage. Although the D and N subpopulations have similar gene expression profiles (Fig. 5C), there are potentially important differences distinguishing these subpopulations, according to the apparent decrease in the D subpopulation and increase in the N subpopulation that were observed as the disease progressed from indolent to acute-type ATL (Fig. 3). Detailed analysis of the genomic and epigenomic differences between these two subpopulations will provide us with information about the genomic and epigenomic lesions that are involved in disease progression. Another important finding is that the expression profiles of cells in the N subpopulation of indolent and acute-type ATLs showed significant differences, even though the majority of the genes were common to both groups (Fig. 5D). Characterization of the genes that show distinct expression patterns will reveal the molecular events that contribute to the progression from indolent to aggressive ATLs.

To address whether the emerging molecular hallmark of ATL was conserved in the novel subpopulations identified, we examined the miR-31 level and *Helios* mRNA pattern in sorted subpopulations (Fig. 6). Through integrative analyses of ATL cells, we recently showed that the expression of miR-31, which negatively regulates noncanonical NF-κB signaling by targeting NIK, is genetically and epigenetically suppressed in ATL cells, leading to persistent NF-κB activation, and is thus inversely correlated with the malignancy of the cells (31). The miR-31 levels in the P subpopulations in asymptomatic carriers and indolent ATLs were as high as those in normal P subpopulations, PBMCs, and resting T cells, whereas those in the D subpopulations decreased significantly and those in the N subpopulations were as low as in acute-type N subpopulations (Fig. 6A). Previously, we also identified ATL-specific aberrant splicing of *Helios* mRNA and demonstrated its functional involvement in ATL (32). As shown in Fig. 6B, the *Hel-2* type variant, which lacks part of exon 3 and thus lacks one of the four DNA-binding zinc-finger domains, accumulated in the D and N subpopulations of asymptomatic carriers and indolent ATLs, and was dominantly expressed in the N subpopulation of acute-type ATLs. Collectively, the molecular abnormality of ATL cells became evident in the gradual progression from P to D to N, even in asymptomatic carriers, strongly supporting the notion that the CADM1/CD7 expression pattern correlates with the multistep oncogenesis of ATL.

One of the more remarkable findings in the expression profile analysis was that the D and N subpopulations of asymptomatic carriers clustered within the same group as those of the indolent ATL cases (Fig. 5A and B). The asymptomatic carriers used in this analysis had high PVLs and relatively high proportions of the D and N subpopulations (Supplementary Table S1). In addition, mono- or oligoclonal expansion of the HTLV-I–infected cells was demonstrated in these cases. HTLV-I–infected cells in the D and N subpopulations of these asymptomatic carriers comprise clonally expanding cells that are potentially at the premalignant and intermediate stages according to their clonality, comprehensive gene expression profile, miR31 expression, and aberrant RNA splicing, all indicating that they can be categorized as asymptomatic carriers with high risk of developing into ATL, requiring careful follow-up (15, 30, 33, 34). Our flow-cytometric analysis of PBMCs from asymptomatic carriers using the CADM1 versus CD7 plot may provide a powerful tool for identifying high-risk asymptomatic carriers. Certain indolent ATL cases are difficult to distinguish from asymptomatic carriers, according to Shimoyama's criteria based on the morphologic characteristics determined by microscopic examination. Characterization of peripheral blood T cells by the CADM1 versus CD7 plot may provide useful information for clinical diagnosis.

According to Masuda and colleagues, manipulation of *CADM1* gene expression in leukemic cell lines suggested that CADM1 expression confers upon ATL cells tissue invasiveness and a growth advantage (35). The mechanism by which HTLV-I infection regulates CADM1 expression and the significance of CADM1 expression in ATL oncogenesis will require clarification by future studies.

Finally, as summarized in Supplementary Fig. S5, we demonstrated that (1) HTLV-I–infected and clonally expanded cells are efficiently enriched in $CADM1^+$ subpopulations; (2) the proportions of the three subpopulations in the CADM1 versus CD7 plot, discriminated by CADM1 expression and stepwise downregulation of CD7, accurately reflect the disease stage in HTLV-I infection; and (3) the $CADM1^+CD7^{dim/neg}$ subpopulations are at the intermediate stage of ATL progression and can be identified even in asymptomatic carriers. These findings will help to elucidate the molecular events involved in multistep oncogenesis of ATL.

Disclosure of Potential Conflicts of Interest

No potential conflicts of interest were disclosed.

Authors' Contributions

Conception and design: S. Kobayashi, T. Watanabe, K. Uchimaru
Development of methodology: T. Ishigaki, T. Yamochi, N. Watanabe